Detection of COVID-19 infection in nasal breath by gas chromatography coupled ion mobility spectrometry (GC-IMS)

Will, Margarete Mirjam

UNIVERSITY OF SPLIT
SCHOOL OF MEDICINE

Margarete Mirjam Will

DETECTION OF COVID-19 INFECTION IN NASAL BREATH BY GAS CHROMATOGRAPHY COUPLED ION MOBILITY SPECTROMETRY (GC-IMS)

Diploma thesis

Academic year:
2023/2024

Mentor:
Prof. Johannes Brachmann, MD

Coburg, August 2024

TABLE OF CONTENTS

ACKNOWLEDGMENT

First of all, I would like to thank my mentors,
Prof. Johannes Brachmann, MD for the constant effort he puts in our Medical School and us students, and especially
Claus Steppert, MD for providing this fascinating topic and being a helpful and patient supervisor during our sample collection and the writing process.

Also, I want to express my gratitude to my colleagues Theresa Molitor and Julia Zeitler, who were part of the study team and participated in the sample collection.
A special thank you goes to Theresa for offering her help also after her part of the study was done.

My thanks extend to all my colleagues who accompanied me during the last six years and have become a second family to me, especially during our time in Split.

My deepest gratitude goes to my parents for everything they have ever done for me. They have always believed in me and without their unconditional love and constant support, emotionally and also financially, I would not have become the person I am and the doctor I will be.

Last but not least I want to thank my boyfriend, who always has an open ear for however small the problem is, who never stops to encourage me and who has become an indispensable person in my life.

LIST OF ABBREVIATIONS

ACE2 – angiotensin-converting enzyme 2

AD – anno domini

AIDS – acquired immune deficiency syndrome

AKI – acute kidney injury

ALDH – aldehyde dehydrogenase

Ang 1 – Angiotensin 1

ARDS – acute respiratory distress syndrome

ATP – adenosine triphosphate

CDC – Centers for Disease Control and Prevention

cDNA – complementary deoxyribonucleic acid

CLIA – chemilumnescent immunoassay

COVID-19 – Coronavirus disease 2019

CT – cycle threshold

CSC – cancer stem cells

CYP – cytochrome P

dt – drift time

ECG – electrocardiogram

ELISA – enzyme-linked immunosorbent assay

EPA – United States Environmental Protection Agency

EUA – Emergency Use Authorization

EVAg – European Virus Archive

FDA – United States Food and Drug Administration

GC – gas chromatography

GC-MS – gas chromatography coupled mass spectrometry

GC-IMS – gas chromatography coupled ion mobility spectrometry

GM-CSF – granulocyte-macrophage colony-stimulating factor

HIV – human immunodeficiency virus

HLA – human leukocyte antigen

IL-1, IL-6 – interleukin-1, interleukin-6

IFN- γ – interferon- γ

kPa – kilopascal (international unit for pressure)

MBq – megabecquerel (international unit for radioactivity)

MHC – major histocompatibility complex

MS – mass spectrometry

MSE – mean squared error

NAAT – nucleic acid amplification test

NCI – national cancer institute

NIH – national institute of health

NRS – non-randomized controlled study

NSP – non-structural protein

PAI-1 – plasminogen activator inhibitor-1

RA – retinoic acid

RBD – receptor-binding domain

RdRP – RNA-dependent RNA polymerase

RAAS – renin-angiotensin-aldosterone-system

RNA – ribonucleic acid

ROS – reactive oxygen species

rt – retention timed

RT-qPCR – quantitative reverse transcription polymerase chain reaction

SARS-CoV-2 – severe acute respiratory syndrome coronavirus 2

SD – standard deviation

SIRS – systemic inflammatory response syndrome

SpO2 – oxygen saturation

SVOC – semi-volatile organic compound

TAT – turnaround time

TIC – tumor-initiating cells

TMPRSS2 – host transmembrane serine protease 2

TNF- α – tumor necrosis factor- α

V/cm – volt per centimeter (unit of an electric field in vacuum)

VOC – volatile organic compound

VVOC – very volatile organic compound

WHO – World Health Organization

1. INTRODUCTION

1.1 Pandemics through history

1.1.1 Definition and origin of pandemics

Before delving into the specifics of pandemics, it is useful to clarify the term itself and distinguish it from other epidemiological vocabulary. According to the Centers for Disease Control and Prevention (CDC), an "endemic" refers to the constant presence and/or usual prevalence of a disease or infectious agent within a specific geographic area. An "epidemic" is defined as a sudden increase in the number of cases of a disease above what is normally expected in that population and area. A "pandemic" instead is described as an epidemic that has spread across multiple countries or continents, typically affecting a large number of people (1).

Pandemics have been a recurring force throughout human history, shaping societies, economies, and even the course of civilizations. These widespread outbreaks of infectious diseases have left indelible marks, not only in terms of mortality but also in their profound socio-economic impacts.

Pandemics can originate from various sources, often involving complex interactions between humans, animals, and the environment. More than two-thirds of emerging infectious diseases are zoonotic, meaning that an infectious agent is transmitted from an animal to humans where it causes disease (2). Wolfe *et al.* outlined a progression through five stages in which a pathogen that originally infects only animals evolves to infect humans, as shown in Figure 1. Stage 1 involves a disease that is transmitted exclusively among animals. In stage 2, the pathogen jumps from animals to humans. Stage 3 sees limited human-to-human transmission, while stage 4 involves more substantial human-to-human transmission and increasing outbreaks. Finally, in stage 5, the disease is transmitted exclusively from human to human (3). The spread of these diseases is often driven by human activities that disrupt natural ecosystems, such as deforestation, agricultural intensification, and climate change, which alter the habitats of various wildlife species and bring humans into closer contact with potential animal hosts (4,5).

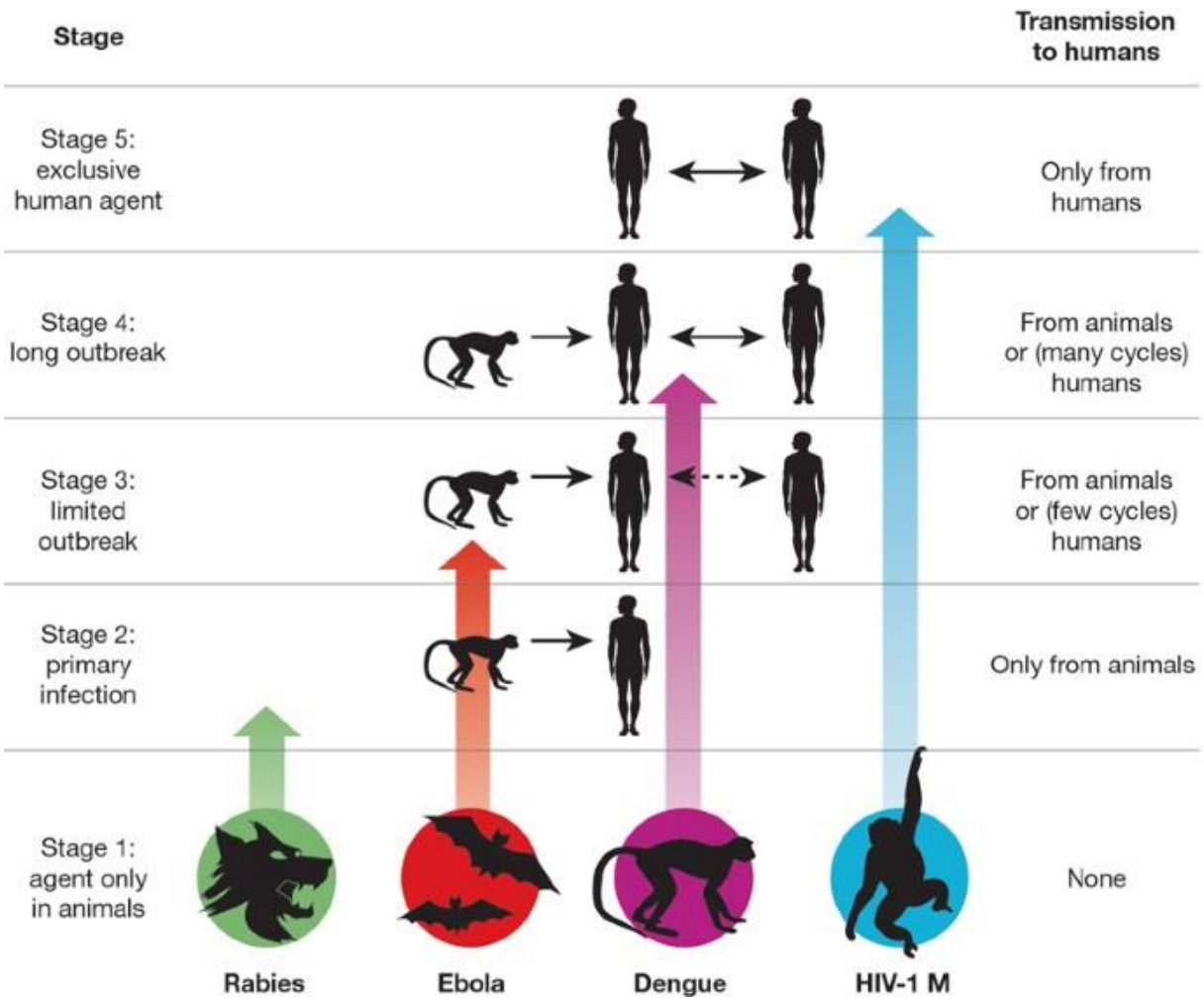

Figure 1. Stages of transmission described by Wolfe *et al.* (2)

1.1.2 Examples from history

One of the earliest and most devastating pandemics was the "Plague of Justinian", which struck the Byzantine Empire in 541 AD. Believed to be caused by the same bacterium as the Black Death, Yersinia pestis, this plague decimated the population, killing an estimated 100 million people, or about half of Europe's population at the time. Its effects were far-reaching, contributing to the weakening of the Byzantine Empire and significantly impacting the course of European history (6).

The "Black Death" of the 14th century remains one of the most infamous pandemics. Sweeping through Europe, Asia, and North Africa, it killed an estimated 200 million people and around 30% of the European population. The high mortality rate resulted in severe labor shortages, which altered the socio-economic structure of Europe, leading to the decline of the feudal system and paving the way for the Renaissance and modern age (7).

In the early 20th century, the “Spanish Flu” of 1918-1919 emerged as one of the deadliest pandemics, infecting a third of the global population and causing at least 50 million deaths. Its rapid spread was facilitated by the movement of troops during World War I, and its high mortality rate disproportionately affected young adults, causing profound demographic and economic disruptions (8).

More recently, the “HIV/AIDS pandemic”, which began in the late 20th century, has had a lasting global impact. With over 36 million deaths and millions more living with the virus, HIV/AIDS has particularly devastated sub-Saharan Africa, affecting not only health but also economic and social structures in the region (9).

Throughout history, pandemics have underscored the importance of public health infrastructure, scientific research, and international cooperation in managing and mitigating the impacts of widespread infectious diseases. They serve as stark reminders of the interconnectedness of human societies and the perpetual challenge of infectious disease control.

1.2 COVID-19 as a modern pandemic

The ongoing “COVID-19 pandemic” has highlighted the modern world's vulnerability to infectious diseases. Since its emergence in late 2019, COVID-19 has caused millions of deaths and widespread economic disruption, prompting unprecedented public health responses and accelerating the development and deployment of vaccines.

1.2.1 Etiology and viral entry into the human body

COVID-19, caused by the novel coronavirus SARS-CoV-2, has its origins in zoonotic transmission, most likely from bats. SARS-CoV-2 is part of the Severe acute respiratory syndrome-related coronavirus species, the only member of the Sarbecoviruses subgenus that is primarily found in horseshoe bats (10). The single-stranded, positive-sense virus has a large RNA genome of approximately 30,000 nucleotides. Alltogether it encodes 16 non-structural proteins (nsp1-16), four structural proteins (Spike (S), Envelope (E), Membrane (M), and Nucleocapsid (N)), and six accessory proteins (ORF3a, ORF6, ORF7a, ORF7b, ORF8, and ORF10). The structural proteins are key components of the virus particle, while the non-structural and accessory proteins play crucial roles in the replication process of the virus’ RNA within the host cell by various mechnisms (11,12). Its replication relies on the RNA-dependent RNA polymerase (RdRP) complex, composed of nsp12 and its cofactors nsp7 and nsp8, and a

proofreading enzyme called exoribonuclease (ExoN), which is one of two domains of nsp14. This combination, along with the virus's discontinuous transcription, leads to high rates of genetic recombination, insertions, deletions and point mutations, making it an ideal candidate for the emergence of a novel disease like COVID-19. Figure 2 shows a schematic presentation of the viral genome of SARS-CoV-2 and its structural proteins.

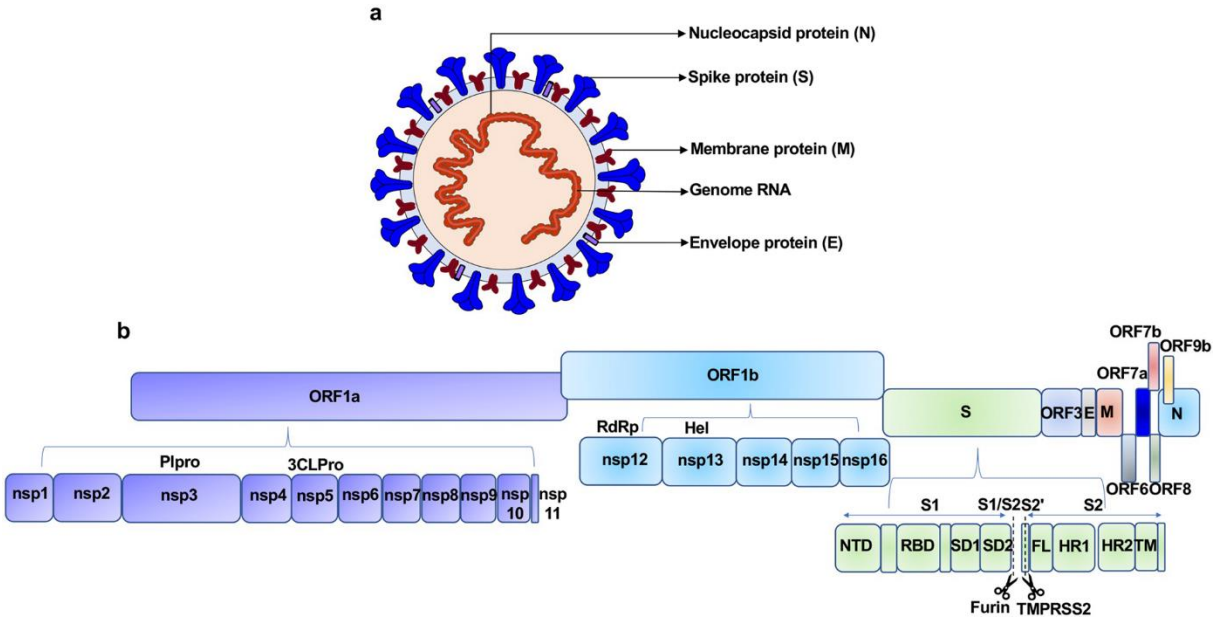

Figure 2. Schematic presentation of SARS-CoV-2 structural proteins and genome (13)

SARS-CoV-2 primarily spreads through respiratory droplets during close contact with infected individuals and via airborne aerosols. Fecal-oral transmission or from mother to child during pregnancy and birth are other possible routes that have been reported in different studies (14,15,16).

The virus enters the human body by firstly binding the receptor-binding domain (RBD) of the Spike protein (S1) to human host cell adaptors. One of the most important ones to mention is the angiotensin-converting enzyme 2 (ACE2) receptor, primarily found in the respiratory epithelium. Other tissues expressing ACE2 receptors include the upper esophagus, the small intestine, myocardial cells, and vascular epithelium, the proximal tubules in the kidneys, urothelial cells in the bladder, and the testis, explaining various symptoms of COVID-19 disease as mentioned later on (10).

After attachment to the ACE2 receptor, subunit S2 of SARS-CoV-2' spike protein facilitates viral entry into the cell by proteolytic cleavage and catalyzation of host proteases like

host transmembrane serine protease 2 (TMPRSS2), furin or cathepsin B/L. This enables the fusion of viral and host membranes and subsequent release of the viral RNA into the host cytoplasm where the cell's machinery is used for replication and release of viral material (13). This process is shown in Figure 3.

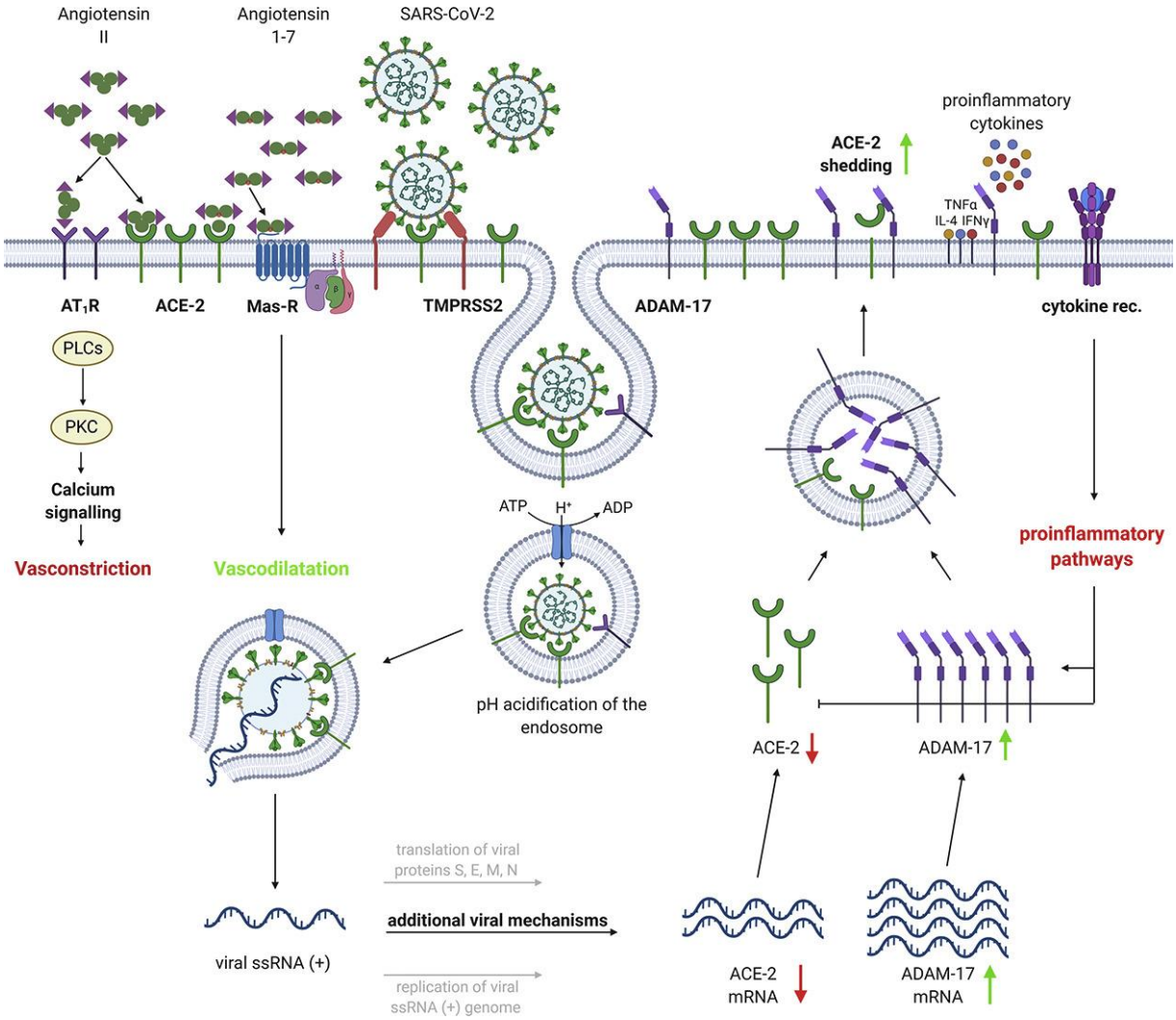

Figure 3. Role of ACE-2 and TMPRSS2 during SARS-CoV-2 infection (14)

1.2.2 Pathophysiology and clinical manifestations

Direct viral damage and perivascular inflammation lead to microvascular injury, increased vascular permeability and microthrombus formation in small capillaries of the lung, eventually contributing to the development of pulmonary edema (10).

In the early phase of the infection, the replication of viral material results in direct damage of the pulmonary endothelial cells causing widespread endotheliitis with subsequent necrosis and cell lysis.

In the late phase, the infected host cells trigger an immune response by recruiting T lymphocytes, monocytes, and neutrophils. By the release of cytokines like tumor necrosis factor- α (TNF-α), granulocyte-macrophage colony-stimulating factor (GM-CSF), interleukin-1 (IL-1), interleukin-6 (IL-6), interferon-γ (IFN)-γ and others, both local and systemic inflammation is caused, in severe cases, this is called “cytokine storm”. The inflammatory cytokines and immune cells, together with vasoactive and histotoxic mediators like reactive oxygen species (ROS) enhance the loosening of inter-endothelial junctions of pulmonary endothelial cells and promote increased vascular permeability and leakage (10,13,15).

Additionally, increased binding of ACE2-receptors by the virus favors a dysregulation of the renin-angiotensin-aldosterone-system (RAAS) (10,15). The RAAS is a regulatory pathway that maintains vascular function, blood flow, and blood pressure. Low sodium, as well as low perfusion pressure at the juxta-glomerular apparatus, trigger the release of renin from the kidneys, which converts angiotensiogen, produced in the liver, into angiotensin (Ang) I. ACE converts Ang I into Ang II, thus promoting vasoconstriction, sodium and water retention and thus a higher blood pressure as well as oxidative stress and proinflammatory responses (17,18).

This is usually counter-regulated by the carboxypeptidase ACE2, a critical enzyme that converts angiotensin II (Ang II) into the vasodilatory and antiinflammatory peptide angiotensin 1-7, playing a key role in cardiovascular and respiratory function. Binding of ACE2 receptors by SARS-CoV-2 blocks them for ACE2 and thereby enhances the effects of Ang II (17). The role of ACE2 in the RAAS is illustrated in Figure 4.

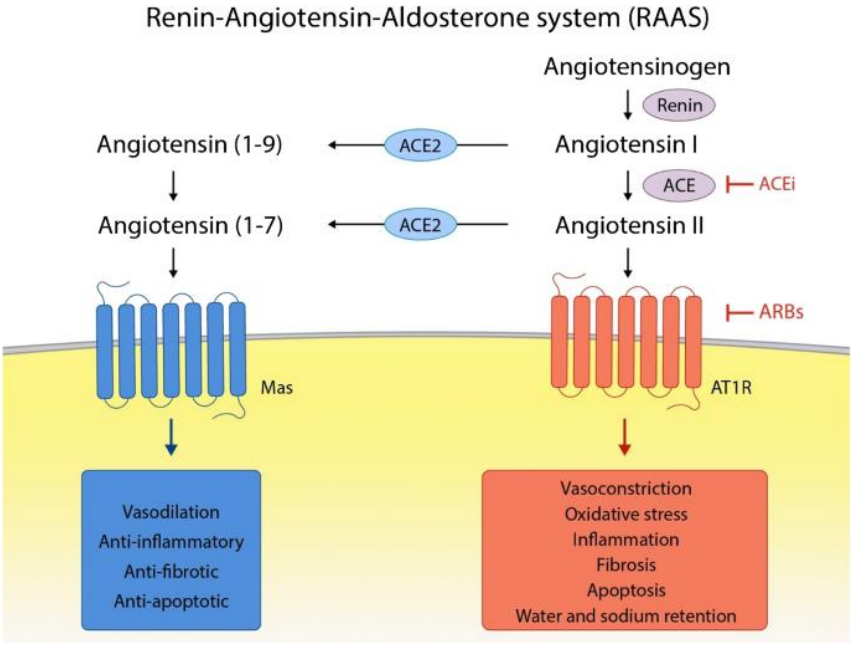

Figure 4. The role of ACE2 within the RAAS (18)

Reduced activity of ACE2 parallelly leads to higher activation of the kallikrein-bradykinin pathway, which is presented in Figure 5. Bradykinin is a vasodilator polypeptide formed by the cleavage of two kininogens by a family of enzymes called kallikreins. It is metabolized by two kininases, one of them also called angiotensin-converting enzyme. Veerdonk *et al.* propose that due to increased binding of ACE2, bradykinin gets less metabolized and contributes to further vasodilation and vascular leakage, enhancing pulmonary edema and other complications (19,20).

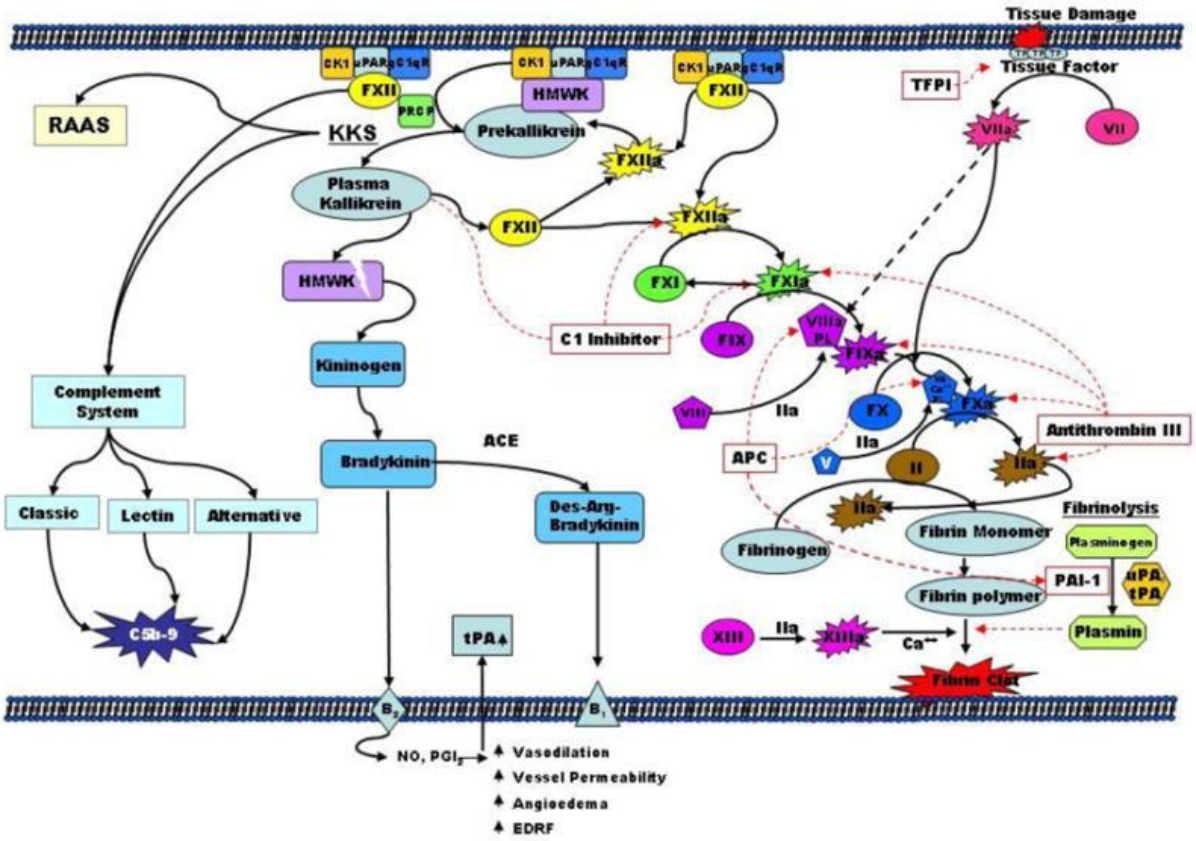

Figure 5. Schematic presentation of the kallikrein system (21)

A variety of extrapulmonary symptoms can occur solely or additionally and comprise mainly the above-mentioned organs which also express ACE2 receptors on their cell surfaces.

Acute cardiac injury, a common complication of COVID-19, has been linked to poor outcomes in severe cases. Heart failure and lethal arrhythmias may contribute to this condition, defined by elevated cardiac troponin (high-sensitivity troponin I) and/or troponin T and abnormalities of ECG or echocardiography (22,23). The myocardial damage is most likely caused by direct viral injury, inflammation, and endothelial dysfunction leading to pulmonary edema and an increased prothrombotic state with possible formation of microthrombi in cardiac vessels (24).

COVID-19 infection also increases the risk of acute kidney injury (AKI) through similar mechanisms. Direct viral injury by binding of the SARS-CoV-2 virus to ACE2 receptors on podocytes and tubular epithelial cells of the kidney can cause cytotoxic effects and inflammation with coagulopathy and hemodynamic instability due to local disruption of the RAAS. Collectively, these factors lead to tubular injury, endothelial damage, rhabdomyolysis and microvascular thrombosis (25).

Coagulopathy is another major complication of COVID-19 infection. Three main pathological mechanisms identified by Conway *et al.* are vascular endothelial cell dysfunction, a hyper-inflammatory immune response, and hypercoagulability (26). Direct viral impact and cytokines as well as immune cells damage pulmonary and vascular endothelial cells causing increased leakage of tissue factor and von Willebrand factor, both of which activate the coagulation cascade by the binding of the clotting factors VII and VIII. At the same time, the fibrinolytic system is slowed down by increased production of plasminogen activator inhibitor-1 (PAI-1) by endothelial cells, macrophages and other cells (27). Cytokines like IL-6 and others promote this release of PAI-1 as well as fibrinogen and von-Willebrand factor. They also stimulate the maturation of megakaryocytes and therefore the production of platelets and even alter platelet function to make them more sensitive to thrombin and platelet activating factor (28). Different mechanisms leading to vascular leakage in COVID-19 infection are illustrated in Figure 6.

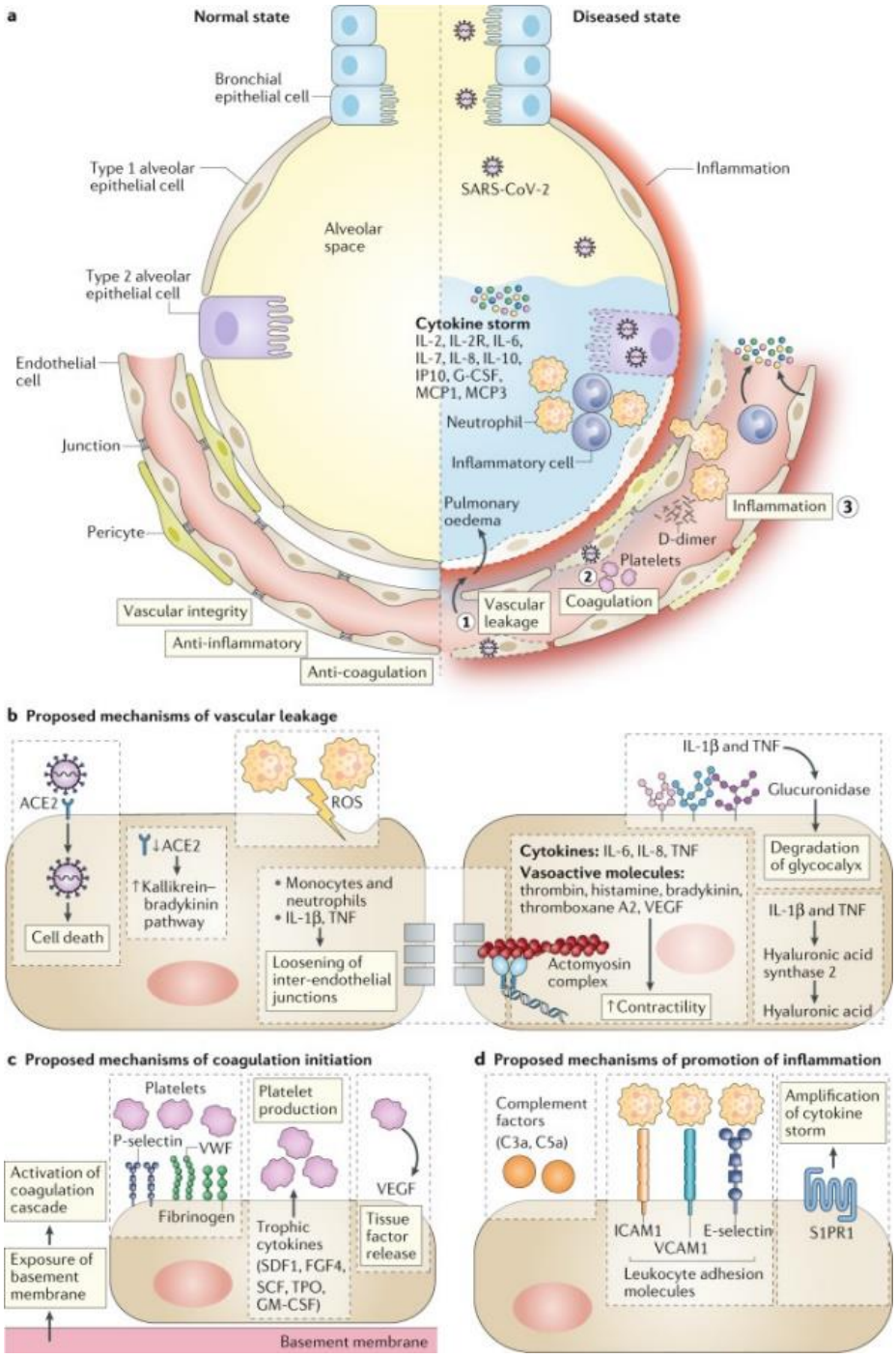

Figure 6. Mechanisms in SARS-CoV-2 infection leading to vascular leakage (15)

1.2.3 Stages of severity and risk factors

In the Coronavirus Disease 2019 (COVID-19) Treatment Guidelines published by the National Institutes of Health (NIH), the clinical spectrum of SARS-CoV-2 infection is divided into five stages: asymptomatic or presymptomatic infection, and mild, moderate, severe and critical illness (29).

Patients with no symptoms who test positive are classified as asymptomatic or presymptomatic, while those with symptoms such as fever and cough but no respiratory distress are considered to have mild illness. Most COVID-19 patients experience only mild symptoms and do not require hospitalization. Around 30% of infected patients remain asymptomatic (29,30). Moderate illness involves evidence of lower respiratory disease with an oxygen saturation (SpO2) of ≥94% (29). Approximately 5% of COVID-19 cases become severe, indicated by an SpO2 <94%, a high respiratory rate or significant lung infiltrates.

Severe COVID-19 disease correlates with elevated levels of proinflammatory cytokines and together with d-dimers they serve as important clinical markers of severity. They often develop acute respiratory distress syndrome (ARDS), systemic inflammatory response syndrome (SIRS) or septic shock, and multiple organ dysfunction/failure with a high fatality rate (24,29). The risk of progressing to severe COVID-19 increases from the age of 50, especially for those aged 65 and above. It is also higher in immunosuppressed, unvaccinated or incompletely vaccinated individuals. Underlying conditions such as cancer, untreated HIV, cardiovascular and chronic kidney, liver or lung diseases as well as diabetes, obesity, pregnancy, smoking and immunosuppressive therapy also elevate this risk (29).

1.2.4 Current diagnostic methods

Today's diagnostic methods for COVID-19 infection primarily include viral tests and antibody tests. An overview is given in Figure 7. Viral tests, such as nucleic acid amplification tests (NAATs) and antigen tests, identify current infection by detecting a part of the virus itself. Antibody or serology tests, such as enzyme-linked immunosorbent assays (ELISAs) or chemilumnescent immunoassays (CLIAs), instead detect specific antibodies targeting parts of the virus. Those can be present during and after infection or may be induced by COVID-19 vaccination (31).

Especially during pandemics, a quick and reliable diagnosis is essential for slowing down the spread of infection and preventing further loss of human and financial resources. Tests should therefore be of high sensitivity and specificity, fast and easy to use and cheap in production. Sensitivity is defined as "the proportion of true positive tests out of all patients with a condition". Specificity instead is "the percentage of true negatives out of all subjects who do not have a disease or condition" (32).

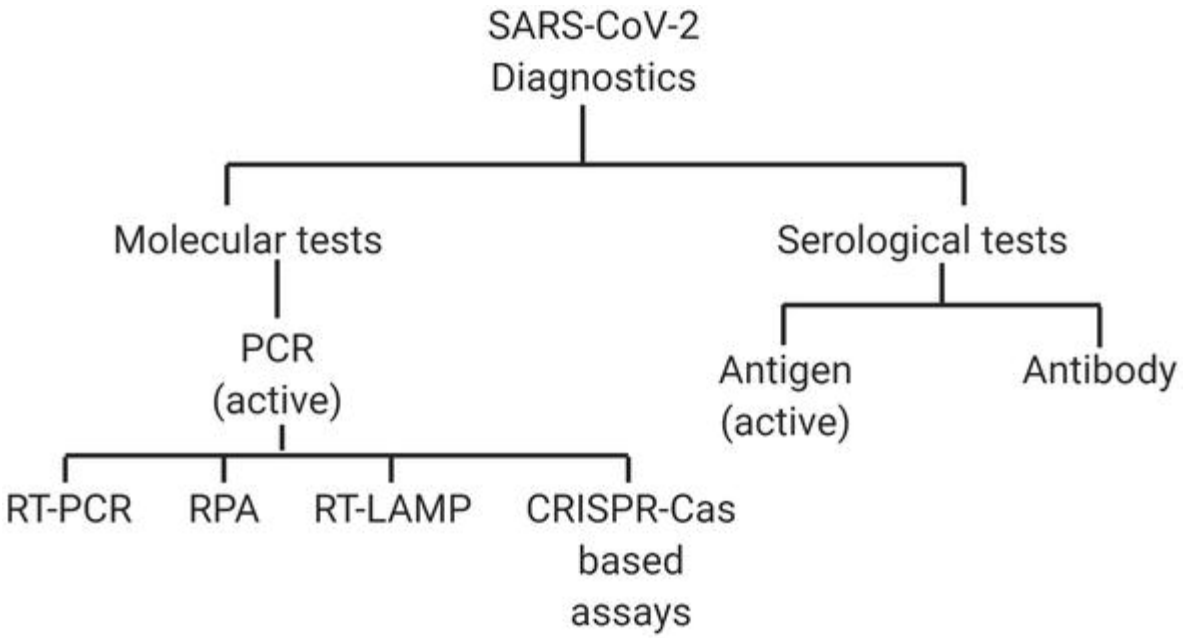

Figure 7. Overview over current diagnostic tests of SARS-CoV-2 (33)

Since NAATs, especially RT-PCR, are considered to have the highest sensitivity for detection of SARS-CoV-2, they are used as primary tool for diagnosis or for confirmation of antigen test results (31,34,35). As the name says, NAATs are used for the identification of viral genetic material. In case of SARS-CoV-2, specimens are usually taken from upper respiratory tract and analyzed for viral RNA sequences by amplification via different methods. The most common one is quantitative reverse transcription polymerase chain reaction (RT-qPCR) (31). Since it is considered the gold standard for detection of SARS-CoV-2 and other viruses, this method will be explained in more detail. After collecting a sample from the patient, the first step is to extract the viral RNA by utilizing commercial RNA extraction kits involving cell lysis, RNA binding to a silica membrane, washing and elution of purified RNA. The extracted RNA is converted into complementary DNA (cDNA) with the help of reverse transcriptase enzymes. Common target genes include two RdRP targets (IP2 and IP4), E- (envelope), N- (nucleocapsid) and S- (spike) genes, made available in January 2020 by the WHO and the European Virus Archive (EVAg) online catalogue (36). Next, the cDNA needs to be split up again by denaturation. Specific regions of the SARS-CoV-2 genome are amplified by mixing the single cDNA strands with primers binding to a certain genetic sequence of the virus and therefore initiating the amplification. This is also called the annealing phase. Other ingredients are nucleotides as substrates for new RNA strands, a buffer and a DNA polymerase, usually Taq polymerase, as the tool for creating new viral genetic material. During extension, fluorescent dyes are attached to the DNA which serve as markers of successful duplication and can be

detected in real time. A number of thermal cyclings is being performed, each consisting of those three steps: denaturation, annealing and extension (33,37,38,39,40).

The number of cycles needed for the nucleic acid target in the sample to become detectable is called cycle thresholds (CT). A low CT value generally indicates a high viral load (29,37). Figure 8 shows the analysis process of a RT-qPCR test.

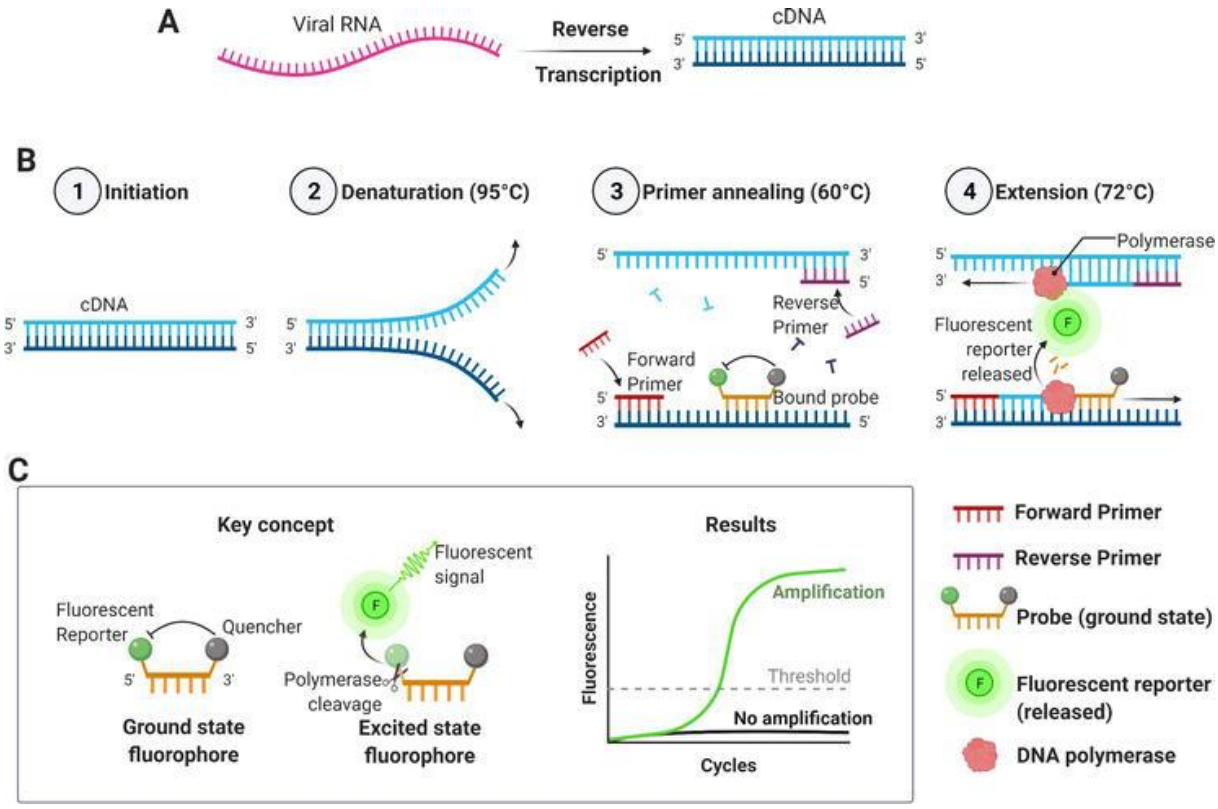

Figure 8. Schematic presentation of the RT-qPCR analysis process (33)

The advantages of this technique are the broad accessibility since it is a standard test used in most laboratories. It is highly specific to the virus and can quickly be modified to new mutations by the use of adapted probes and primers. It also is very sensitive since only one copy of a specific DNA template is needed for amplification. Further, multiple targets can be detected simultaneously and no purification step is needed in RT-PCR.

Disadvantages are the long turnaround-time (TAT) up to 24 hours, which is the time it takes until a clear result can be given (33,38). Compared to rapid antigen tests it is also more expensive and requires expert staff for processing the probe. Of course, as in almost any test there is the possibility for the probe to get contaminated or for errors in the amplification phase, which can lead to inaccurate or false results (38).

As being said before, in the face of a pandemic a fast and easy to use test, which is still reliable and in the best case cheap to purchase, has still not been found. The idea for this study was to detect COVID-19 in the breath of patients by a non-invasive method, which can be performed by untrained staff in less than two minutes. The next chapter gives an introduction into the chemical and biological background of the particles being measured and the device we used for measurement.

1.3 Volatile organic compounds (VOCs)

1.3.1 Definition and sources of VOCs

In 2010 the European Union released the "Industrial Emissions Directive" (IEA) in which VOCs are defined as "any organic compound as well as the fraction of creosote[1], having at 293,15 K a vapour pressure of 0,01 kPa or more, or having a corresponding volatility under the particular conditions of use" (39).

Based on their range of boiling points, the WHO and EPA further subdivide VOCs into very volatile (gaseous) organic compounds (VVOC), volatile organic compounds and semi volatile organic compounds (SVOC). An overview together with some examples for each category is given in the table below (Figure 9) (40).

Description	Abbreviation	Boiling Point Range (°C)	Example Compounds
Very volatile (gaseous) organic compounds	VVOC	<0 to 50-100	Propane, butane, methyl chloride
Volatile organic compounds	VOC	50-100 to 240-260	Formaldehyde, d-Limonene, toluene, acetone, ethanol (ethyl alcohol) 2-propanol (isopropyl alcohol), hexanal
Semi volatile organic compounds	SVOC	240-260 to 380-400	Pesticides (DDT, chlordane, plasticizers (phthalates), fire retardants (PCBs, PBB))

Figure 9. Subdivisions of VOCs with examples (40)

[1] a dark brown oil containing various phenols and other organic compounds, distilled from coal tar and used as a wood preservative

The “United States Environmental Protection Agency” (EPA) defines VOCs as “any compound of carbon excluding carbon monoxide, carbon dioxide, carbonic acid, metallic carbides or carbonates and ammonium carbonate, which participates in atmospheric photochemical reactions, except those designated by EPA as having negligible photochemical reactivity” (40). Another article on the same webpage further describes them as “compounds that have a high vapor pressure and low water solubility”, which are “emitted as gases from certain solids or liquids” (41). Those solids or liquids include chemicals like cosmetic products, cleaning supplies, paints, aromas in food and drinks, and building materials as well as office materials like glues, permanent markers, and printers (42).

Yadav and Pandey categorized sources of VOCs as natural or anthropogenic. Anthropogenic are all before mentioned sources of VOCs, as well as agricultural waste, pesticides, or many examples from industrial processes. Natural sources include emissions from trees and plants, natural forest fires, and bog landscapes as well as products of biological processes in animals, humans, and microbes (43).

1.3.2 Chemical background

To understand the concept of volatile organic compounds it is helpful to review basic principles of organic chemistry and the subdivision of chemical elements according to their functional groups.

An organic compound is any molecule containing carbon atoms covalently bound to other atoms (44). A functional group is made out of one or more atoms within these molecules and determines their chemical properties (45). Those molecules of each group, which evaporate at room temperature or at a pressure of 0.01 kPa, are called volatile and together they comprise our group of interest, the VOCs. They are small, non-charged molecules varying in lipophilicity and volatility according to their combination of atoms; the more carbon and other atoms they have, the more lipophilic and the less volatile they are (46). Figure 10 shows an overview over the most common functional groups of organic compounds.

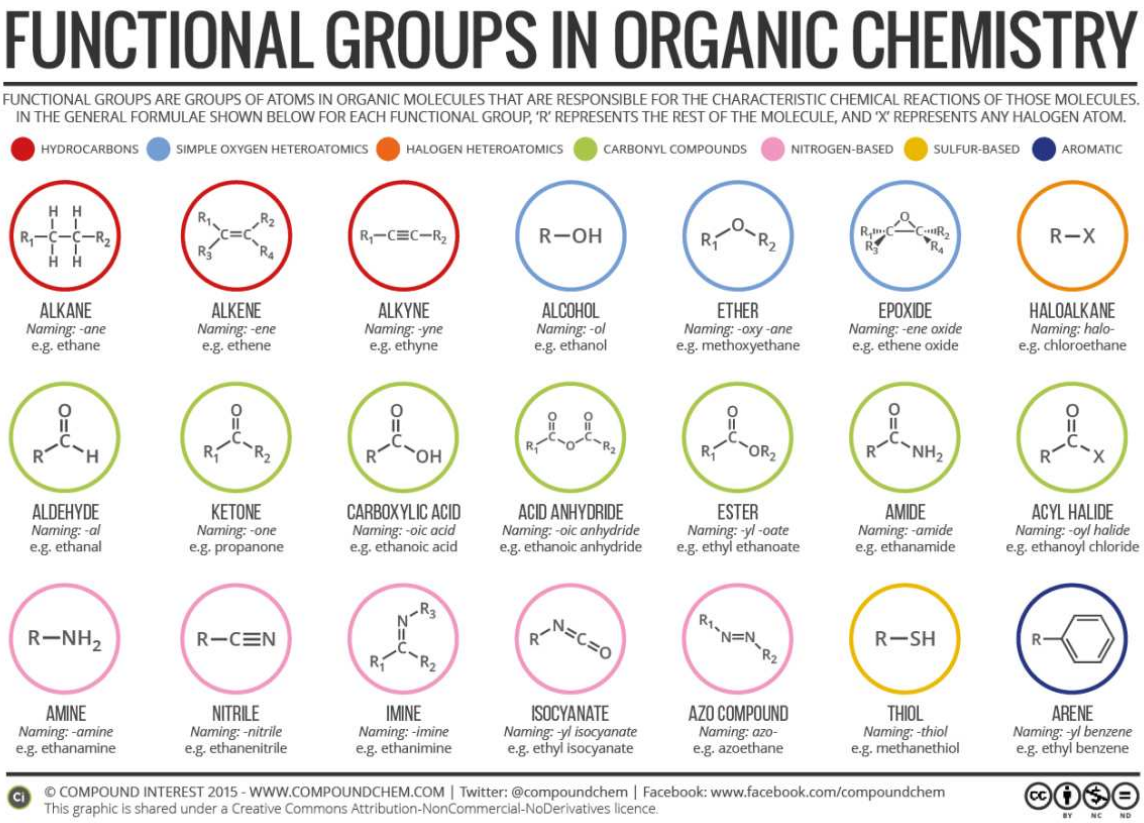

Figure 10. Overview over some functional groups in organic chemistry (47)

The basic group of organic compounds are the hydrocarbons, made out of carbon and hydrogen atoms. Figure 11 shows how they are subdivided based on their form, which is either open chain/aliphatic or ring/cyclic. Aliphatic compounds are further divided by their type of covalent bond and thus named differently. Molecules with a single bond between carbon atoms are called alkanes, those with double bond alkenes, and with triple bonds they are alkynes. Cyclic compounds can either be homocyclic, with their ring made purely out of carbon atoms, or heterocyclic, with their ring containing at least one other atom as carbon. Homocyclic compounds are grouped into alicyclic or aromatic. The basic aromatic hydrocarbon is benzene.

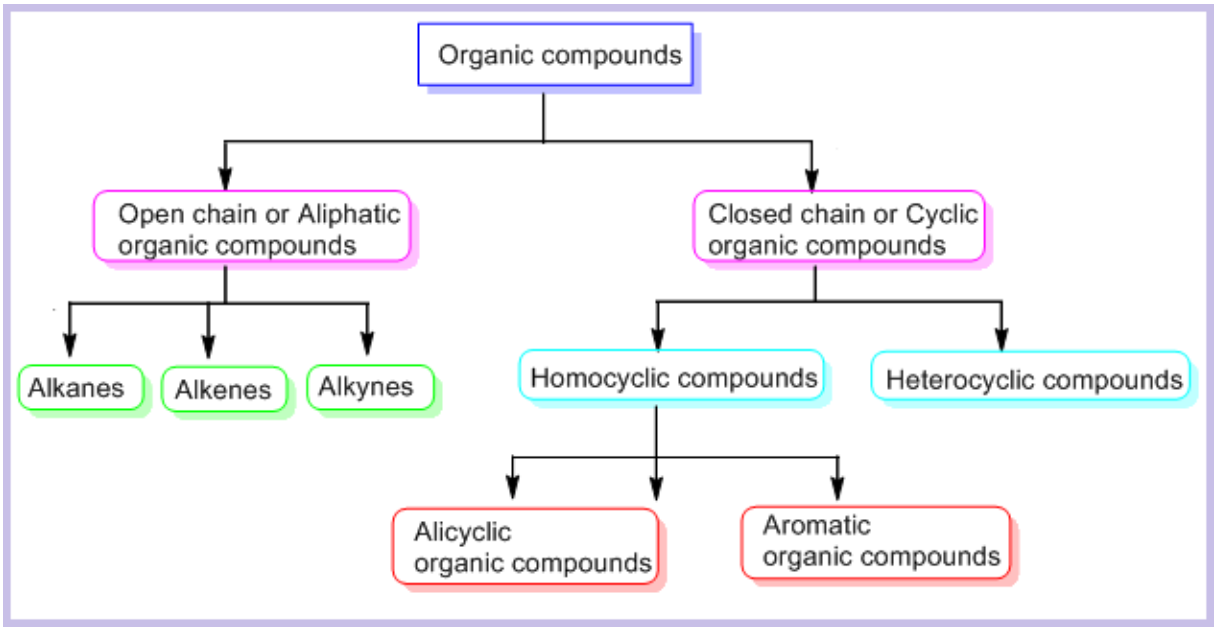

Figure 11. Division of organic compounds according to their structure (45)

If one or more hydrogen atoms are replaced by halogens the molecules are called halocarbons. These include fluorine, chlorine, bromine, iodine, astatine and tennessine and are often man-made (48).

Carbonyl compounds are another important group of organic molecules. Here, an oxygen atom is bound to one of the carbon atoms by a double bond. Depending on which atoms the two free bonds of the carbonyl group are bound to, we get for example ketones - both of the other attached groups are carbon groups -, aldehydes, one of the carbon groups is replaced by a hydrogen atom - or other molecules (49).

The biggest groups of VOCs comprise aliphatic and aromatic hydrocarbons, halocarbons, alcohols, ethers, esters, ketones and aldehydes (46). A complete list of VOCs released by the Ontario's Ministry of Environment as well as an overview over the correlation of single VOCs with certain diseases are already available for public use online (50,51).

Irga *et al.* listed the 20 most common VOCs emitted by humans as shown in Figure 12. Aldehydes comprised the biggest group of identified VOCs, followed by ketones and alkanes (52).

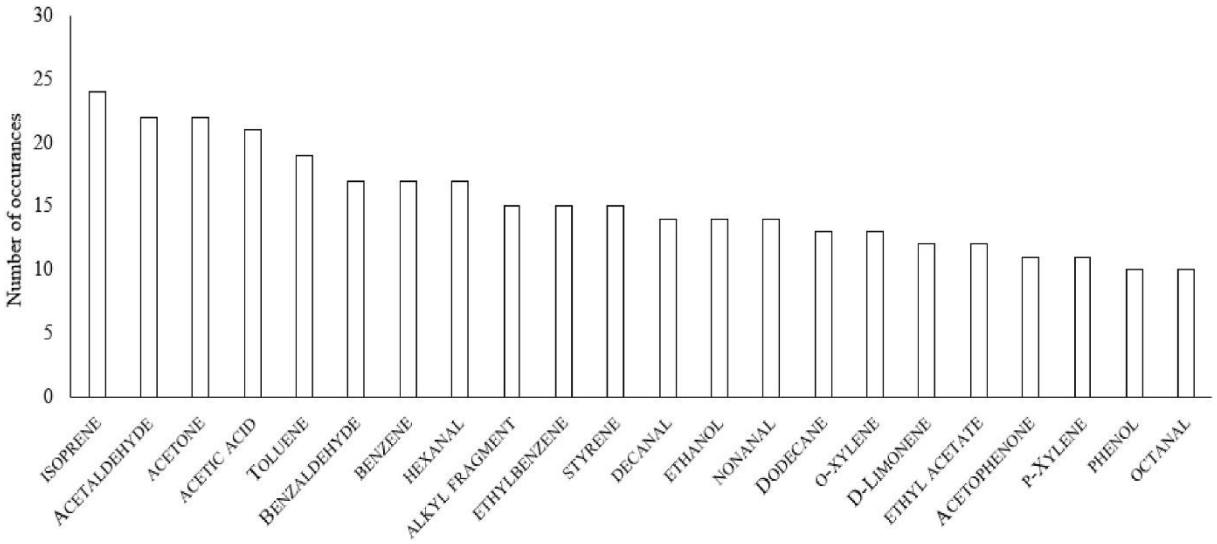

Figure 12. 20 most common VOCs emitted by humans (52)

1.3.3 The human volatilome

As mentioned above, the human body can also produce and release VOCs as a result of different metabolic processes, some of which can be perceived as a specific smell.

These odorous VOCs have played an important role in prelaboratory medicine and have – among others – been described by Hippocrates, Galen, and Paul of Aegina, when doctors had to rely solely on their senses to make a diagnosis. This included the general appearance and obvious signs of disease, but also the taste and smell of breath, sweat, urine, or feces of patients and their wounds. We now know that the "rotten apple" smell in the breath of diabetic patients is caused by a higher concentration of ketones in their bodies and the sweet smell of urine by an increased excretion of glucose which cannot be taken up into body cells. Advanced liver disease is characterized by a "fetor hepaticus", the result of excessive accumulation of C2-C5 aliphatic acids and methylmercaptan. Experienced medical staff may even be able to tell the causative agent of an infection by its smell. Common examples are *Clostridium difficile*, *Pseudomonas aeroginosa* or *Staphylococcus aureus* (53,54).

Pauling *et al.* were one of the first ones to examine the composition of the human breath by gas chromatography (GC) and since then more effort has been made to study endogenous volatile compounds of the human body (55). In 2014, de Lacy Costello *et al.* published a compedium of 1840 VOCs, detected in breath, saliva, blood, milk, skin secretions, urine and feces of healthy individuals. Notably, breath VOCs overlap significantly with other body fluids, especially feces. This is particularly noteworthy considering their different origins - breath VOCs typically arise from body cells and potentially infectious agents and fecal VOCs mainly

from gut bacteria (56,57).

The difference in VOC composition of various body compartments has been the focus of even more studies, mainly with the purpose of finding biomarkers for specific types of cancer (58,59,60). The National Cancer Institute defines a biomarker as "a biological molecule found in blood, other body fluids, or tissues that is a sign of a normal or abnormal process, or of a condition or disease" (56). Studies on changes of breath VOCs in renal or liver diseases as well as altered fecal VOCs in Alzheimer patients and the differentiation of different strands of bacteria give rise to the hope that VOCs may also serve as potential diagnostic tools in various pathological conditions besides cancer (61,62,63,64). By the use of a similar technique, Steppert *et al.* already demonstrated a different VOC composition in the breath of patients infected with Influenza and SARS-CoV-2, adding viral diseases to the list of potential diagnoses made by VOC analysis (65,66).

However, the fact that VOCs are products of metabolic processes also carries the risk that fluctuations in their composition are caused by physiological conditions and daily activities like dietary alterations, physical activity, smoking, medication use or acute illness (57). Therefore, further research on healthy individuals in different physiological suppositions, e.g. sex, age, physical activity etc., is of utmost importance to provide a panel of "reference values" similar to those existing for conventional biochemical testing of blood, urine etc.

1.3.4 Metabolic processes leading to the formation of VOCs

It may be important to mention that the production of VOCs by the human body happens via physiological as well as pathological metabolic pathways. Different diseases contribute to the formation of distinct VOC profiles, either by changing the concentration of preexisting VOCs or by generating new ones (67). This is similar to the elevated or decreased levels of selected enzymes measured in blood or other body fluids which confirm the presence and stage of certain pathological states. Some examples of metabolic pathways are:

1. Oxidative stress: The presence of reactive oxygen species (ROS) leads to formation of some hydrocarbons by peroxidation of polyunsaturated fatty acids. They upregulate cytochrome P450 (CYP) enzymes which further oxidize the hydrocarbons into alcohols, ketones and aldehydes (57). During ATP production in the mitochondria, ROS are produced as a byproduct of the respiratory chain, having an unpaired electron in their outer shell. They play important roles in cell signaling regarding proliferation, adaption to hypoxic states, inflammation and cell fate determination and are counterregulated by

the presence of antioxidants like vitamins C, D, E and carotenoids. Exogenous sources of ROS include cigarette smoking, pollution and radiation. Excessive amounts, either by overproduction of ROS or descrease of antioxidants, are responsible for irreversible damage and death of cells (67,68,69). Those states of excessive ROS and subsequent damage of surrounding cells by the release of free radicals are called oxidative stress and are linked to a higher risk of chronic inflammatory diseases and cancer development. Altered patterns of VOCs due to these pathways can then be measured in breath, as depicted in Figure 13 (67).

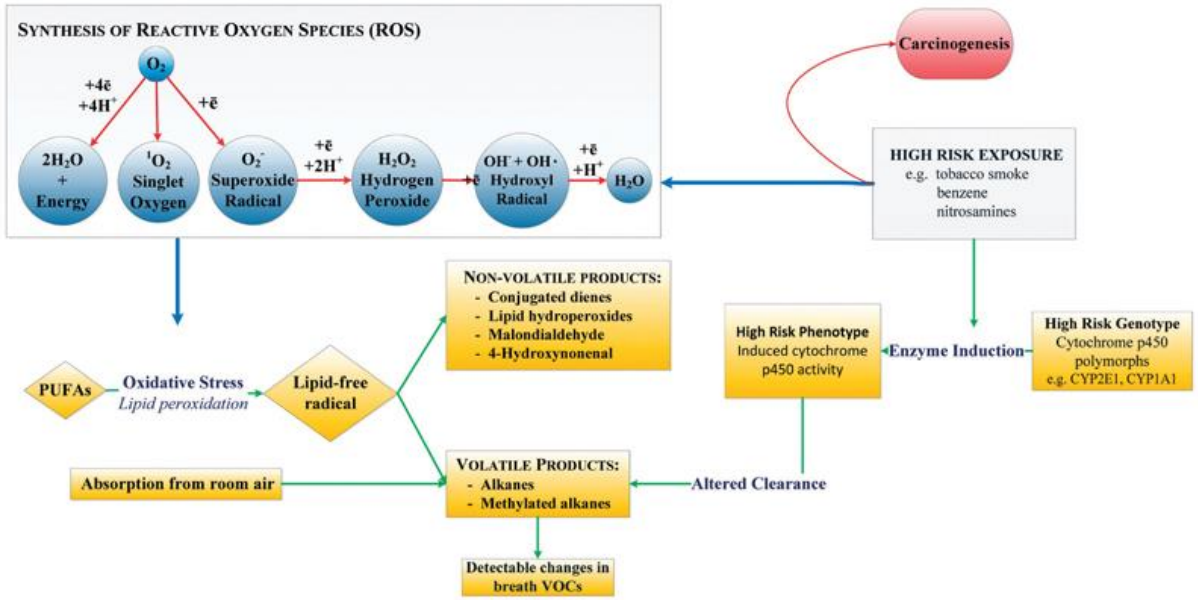

Figure 13. Influence of ROS on VOC composition in breath (67)

2. MHC expression: Aksenov *et al.* demonstrated in vitro that human B-cells produce a certain set of VOCs based on which human leukocyte antigen (HLA) gene-coding region is activated. By the resulting expression of a certain major histocompatibility complex (MHC) class I antigen each cell has their own “fingerprint” helping other immune cells to recognize them as body cells and thereby preventing their degradation (70,71). The HLA gene-coding region plays not only a big role in cellular recognition and immune response but also in the subconscious selection of sexual partners by their organism-specific odor. The production of a certain VOC profile based on the expression of a specific HLA allele may provide an explanation for this (70).

3. ALDH expression in cancer stem cells: Aldehyde dehydrogenase (ALDH) is a family of 19 enzymes which have been identified to play roles in regard to cancer development. Distributed throughout the whole body they are involved in the oxidation of aldehydes. They also function in cellular detoxification processes, metabolism and signaling of retinoic acid (RA), protection against ROS and maintenance of eye health and vision. An overview over signaling pathways and effects of ALDH is given in Figure 14. Malignant tumors generally express a population of cells with stem cell properties, called cancer stem cells (CSC) or tumor initiating cells (TIC), which showed to contain a higher concentration of ALDH proteins. Especially ALDH-dependent RA signaling plays a key role in gene expression, cellular differentiation and therefore tumorigenesis and therapy resistance of cancer cells (72). Brunner *et al.* compared the VOC profiles of in-vitro cancerous and non-cancerous cells and were able to distinguish them clearly. This was mainly due to significant differences in aldehyde levels which were lower in the cancerous cell lines, likely caused by their higher activity of ALDH (73).

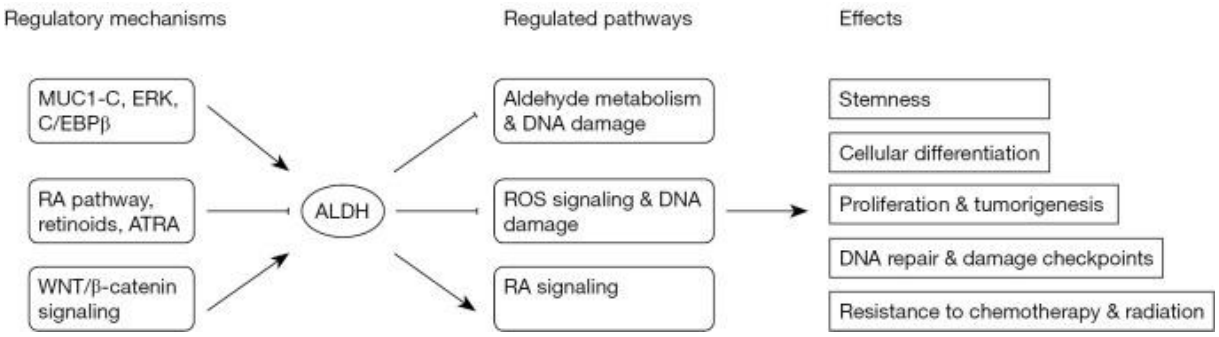

Figure 14. Effects of ALDH on human cells (72)

1.3.5 Detection and analysis of VOCs

Gas chromatophraphy coupled mass spectrometry (GC-MS) is considered to be the gold standard for the analysis of volatile compounds and will thus be explained in more detail in this chapter. It combines the ability of gas chromatography (GC) to separate substances with the detection and identification strengths of mass spectrometry (MS).

In GC, the gaseous mixture is injected into a separation tube, also called “column”. It consists of two phases, a mobile phase containing a so called carrier gas, that accompanies the mixture through a second, the stationary, phase. The stationary phase is made of a high-boiling liquid adsorbed on a solid substance. Each component in the gas has different chemical

properties and affinity for the stationary phase and leaves the column at different times, also called retention times (74,75).

Next, the MS breaks down each molecule into its ionized fragments, which are then accelerated, deflected and finally visualized in form of peaks by a detector. Figure 15 illustrates the principal setup of a classical GC-MS device. Raw data is first depicted on a heat map and must be processed further for analysis. Figure 16 shows various steps of this process, namely denoising, baseline correction, alignment, peak picking and merging of peaks (76). By measuring the mass-to-charge ratio (m/z) of each fragment, molecules of the mixture can be identified on the basis of their molecular weight, elemental composition and chemical structures. Even molecules with similar patterns of ionized fragments in MS can be distinguished by their different retention times due to previous separation in GC. The combination of GC and MS therefore yields a more accurate result and is the preferred method in volatile compound analysis (77).

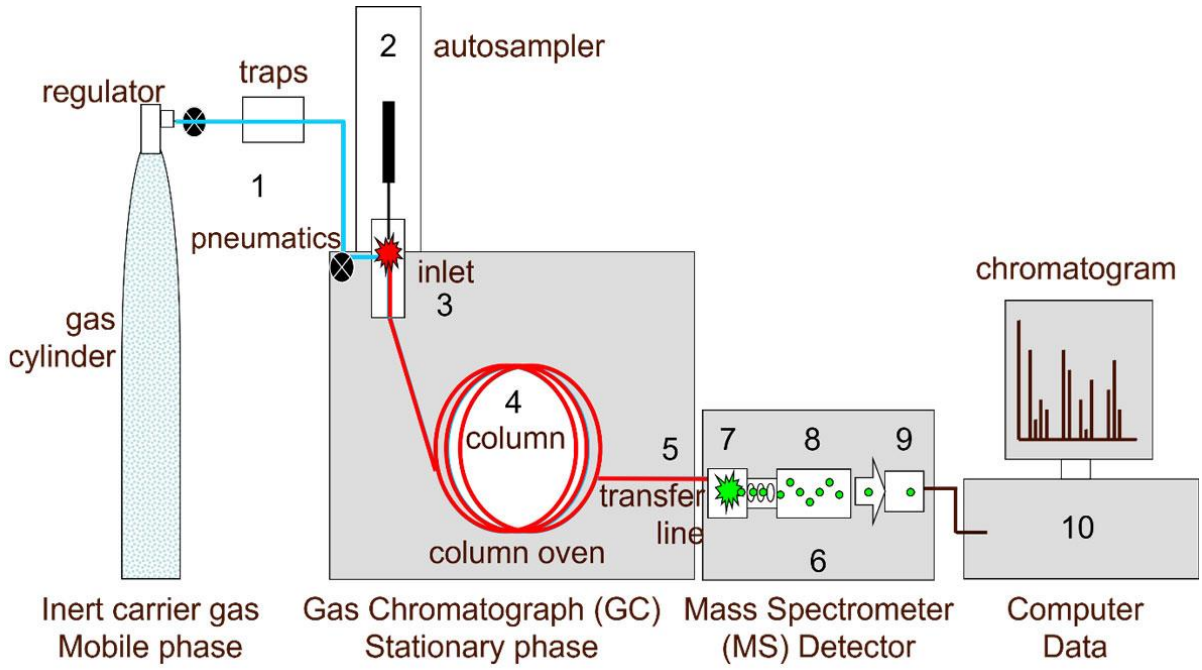

Figure 15. Simplified illustration of a GC-MS device (77)

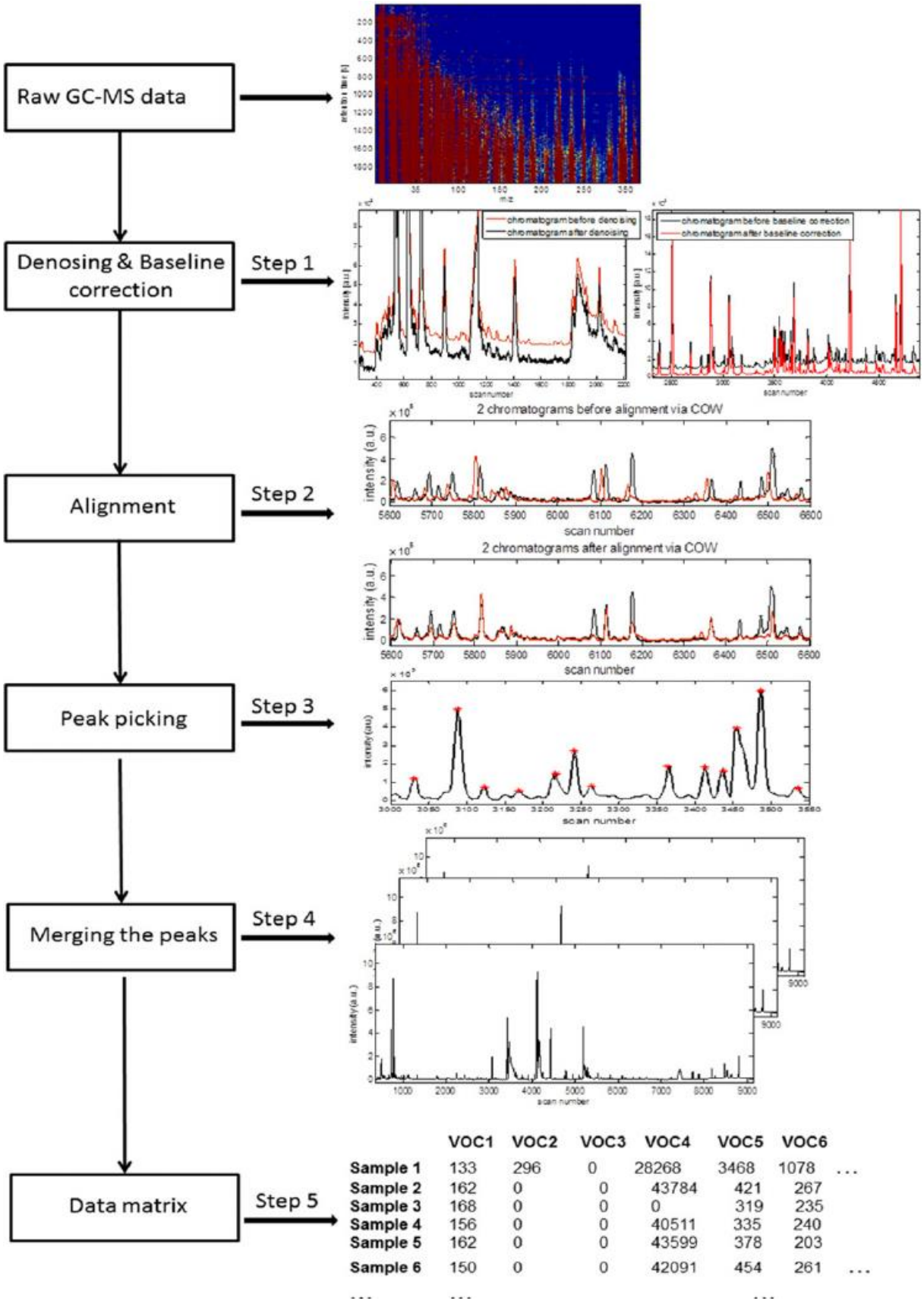

Figure 16. Steps in GC-MS data processing necessary for analysis (76)

Even though GC-MS is still considered gold standard for VOC analysis, gas chromatography coupled ion mobility spectrometry (GC-IMS) has become a popular alternative in recent years.

A standard IMS device, as depicted in Figure 17, consists of an ionization unit, a drift tube filled with gas, and a detector area. Initially, the sample is ionized to create charged particles. An electrical field within the drift tube then forces the ions towards the detector. As the ions traverse the tube, they collide with drift gas molecules, which slow them down before being reaccelerated by the electric field. The larger the ions, the more frequent the collisions, resulting in a slower arrival at the detector. The IMS measures the drift velocity of ions, with longer drift times indicating higher molecular weights, larger surfaces or lower charge (78,79).

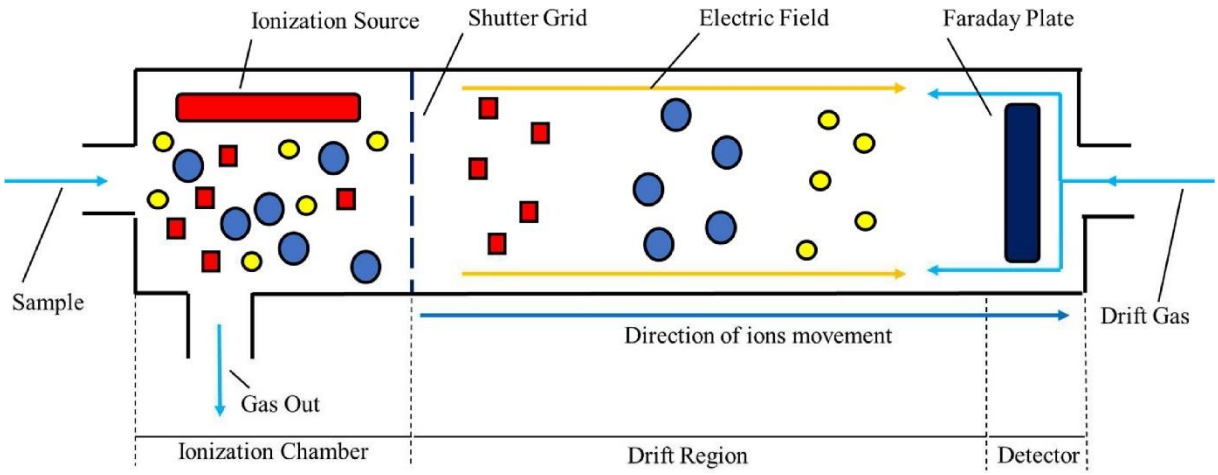

Figure 17. Schematic presentation of a GC-IMS device (80)

IMS operates at ambient pressure and does not need high vacuum. It has traditionally been used in the military field and still is used at airports to screen for explosive substances, chemical warfare agents and illegal drugs. Nowadays, GC-IMS is applied in various fields including food industry, natural product analysis and environmental production (81).

It combines the high separation capability of GC with the quick response of IMS. Even though its relatively new appliance for human VOC analysis corresponds with a small database of identified VOCs, the fast and easy handling of GC-IMS as well as the possibility of a portable device guided our decicion in using this method for our study.

Advantages and disadvantages of GC-MS compared to those of GC-IMS are summarized in Table 1.

Table 1. Comparison of GC-MS and GC-IMS (82,83)

	GC-MS	GC-IMS
Advantages	▪ Widely used, large database ▪ Highly sensitive, accurate and precise, also in complex samples ▪ Many peaks can be assigned to specific substances	▪ Highly sensitive and selective for volatile and semi-volatile compounds ▪ No need for sample enrichment ▪ Requires less energy ▪ Uses non-hazardous solvents, more environmentally friendly ▪ Radioactive ionization sources can be recycled ▪ No carrier gas is needed, works with air ▪ Portable, suitable for in-field analysis ▪ No pretreatment required ▪ Analysis time 3-10 minutes ▪ Lower cost
Disadvantages	▪ Requires high vacuum conditions and energy ▪ Requires helium as carrier gas ▪ Stationary, big ▪ Sample analysis time >30 minutes	▪ Smaller number of qualitative substance in current databases, needed for identification of VOCs

Interestingly, GC-MS is also listed as an Emergency Use Authorization (EUA) product by the United States Food and Drug Administration (FDA) and may even be used as an individual diagnostic breath test and for the detection of COVID-19 by in “near patient / point-

of-care” settings (84). To test wether GC-IMS is also suitable for this purpose was exactly the goal of this study.

2. OBJECTIVES

2.1 Aims of the study

The aim of this study was to assess whether GC-IMS can be used as a reliable screening tool for the detection of COVID-19 in humans and therefore be used as an easily-accessible, faster, non-invasive, and all-in-all cheaper alternative to current testing strategies.

2.2 Hypothesis

Patients, tested positive for COVID-19 by PCR, can be detected by measuring the VOC composition in their nasal breath with GC-IMS.

3. SUBJECTS, MATERIALS AND METHODS

3.1 Study design

This research has been conducted as a non-randomized controlled study (NRS). The exhaled nasal breath of a group of hospitalized patients was tested by GC-IMS and later on analyzed for its composition of VOCs. All measurements took place in the Regiomed Hospital Coburg and were executed between February and July 2022 by three students of the University of Split School of Medicine / Medical School Regiomed.

3.2 Ethical approval

All subjects gave their written informed consent for inclusion before they participated in the study. The study was conducted in accordance with the Declaration of Helsinki. Ethical approval has been given by the ethics committee of the University of Erlangen (Report No 426_18B) on the 16th of December 2020.

3.3 Subjects

A total of 112 patients of mixed age and sex have been tested, using a nasal catheter connected to the GC-IMS device. Data about the first positive COVID-19 test, type and severity of symptoms, possible previous COVID-19 infections, the patients' COVID-19 vaccination status, and the current body temperature of each patient were collected additionally.

Excluded were underaged patients or patients who fulfilled all criteria but could not fully comprehend the aim and concept of the study due to reduced mental state by illness or under the influence of drugs as well as patients with a COVID-19 infection within the last three months for the negative control group. Two patients had to be excluded because of above-mentioned reasons. The patients were divided into two groups, according to their PCR test results which we obtained from the hospital's data software, ORBIS. Inclusion criteria for the test group (n = 66) were a positive PCR test within the last 24 hours before GC-IMS testing, with a CT value below 40. For the control group (n = 44), a negative PCR test within the last 24 hours was necessary, with a CT value of >40 and no COVID-19 infection within the last three months before GC-IMS testing.

In the next step, all patients were tested by the GC-IMS device. Due to errors in measurement and resulting incomplete data, 19 patients had further to be excluded, leaving a study population of 91 patients. To better demonstrate the process of inclusion and exclusion of

patients, a flow diagram according to the CONSORT-criteria of 2010 has been created (Figure 18).

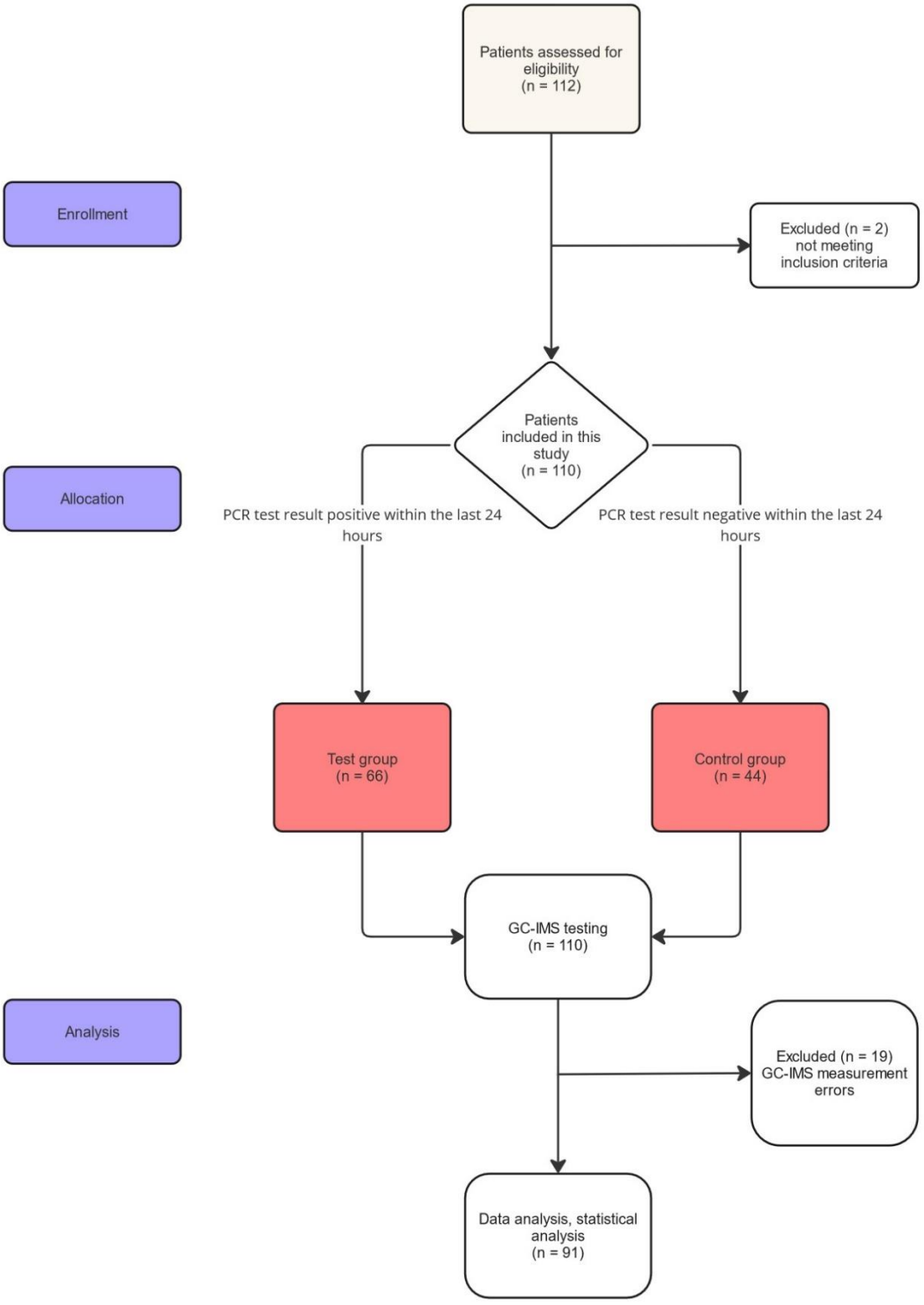

Figure 18. CONSORT flow diagram of the study

3.4 Variables

The constant variables in the study comprised the patients' case numbers in the hospital's internal software and their study participant numbers. The independent variables included patients' age and gender, their PCR test results, and corresponding CT values. The composition and potential clusters of VOCs in the nasal breath served as the dependent variable and primary outcome measure. Different symptoms presented by some patients at the time of measurement, as well as their body temperature, previous COVID-19 infections, and current vaccination status, were considered as confounding variables.

3.5 PCR test

All patients needed to be tested for COVID-19 by a PCR test prior to being measured by GC-IMS. A nasopharyngeal swab was obtained by trained medical staff in the emergency room or on the patients' ward. The testing material was the "Xpert Nasopharyngeal Sample Collection Kit for Viruses" (Cepheid, Maurens-Scopont, France). Further devices comprised the StarMag 96 UniTube Kit, the SGPRep32 extraction system as well as the Allplex 2019-nCoV Assay (all by Seegene, Seoul, South Korea). Targeted genes consisted of the E, N, and RdRP genes.

3.6 Breath sampling and data analysis

Within 24 hours after the PCR test, the exhaled nasal breath of the same participants was analyzed using a mobile GC-IMS device of the technical manufacturer STEP (Sensortechnik und Elektronik Pockau GmbH, Pockau, Germany). For this device, no preanalytical measures are necessary. For the carrier gas in the GC-column and the drift gas in the IMS, is being used with an internal activated carbon filter ensuring equal measurement conditions. An internal pump guarantees the precise filling of a loop with 2 ml of the sample. The 2 ml are then released into the GC by a valve and particles are separated at a temperature of 60°C. Next, the particles are ionized by a weakly radioactive tritium source with less than 100 MBq activity and accelerated by an electrical field (400 V/cm) in a drift-tube of 50 mm in length. The ion gate opens in a pulsatile manner every 30 milliseconds for a duration of 100 microseconds. A heated collector electrode (60°C) captures the ions at intervals of 10 microseconds, according to their drift times after collision with air molecules in the drift tube.

The device has four measurement modes:

- “Auto Sample” for continuous measurement at preset time intervals
- “Trigger Sample” for manual and extern trigger signals
- “Control Sample” with adjustable periodic measurements and breaks and
- “Direct Sample” for continuous measurement with an open valve

The manual mode “Trigger Sample” was selected for our study to ensure that only the specific VOC composition of a participant’s nasal breath is measured in each sample. Since the participants have been isolated due to their possible infectiousness, a mobile GC-IMS device containing a rechargeable lithium-ion battery was used and disinfected after every application.

Prior to measurement, a foam-cuffed nasal oxygen tube (Well Lead Medical Co., Panyu, China) was placed in one nostril of the participants and the other end was connected to the GC-IMS device by a polyethylene pipe and a 5 µm inline filter. Filters were exchanged after every use. Participants were asked to inhale deeply and exhale slowly through the nose. Right before expiration, measurement was started manually by the medical staff and the breath sample was collected for 10 seconds. An integrated mini-computer (pITX with Operating System Windows 7; software: IMS-Control Version 1.1) automatically started the analysis. Within minutes, a preview of the results was already available, as shown exemplarily in Figure 19. Stored data could be extracted at a later point of time.

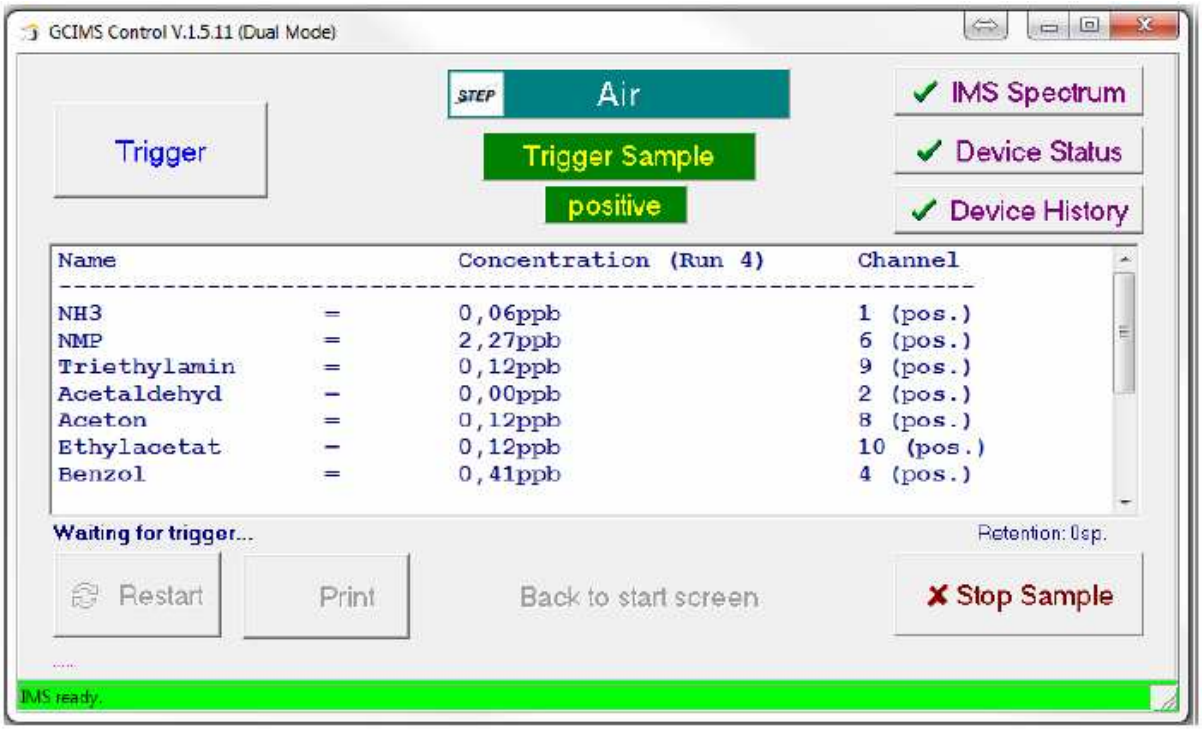

Figure 19. Screenshot of an exemplary measurement in trigger sample mode

The detector captures 16 individual spectra each second which were eventually put together as a denoised spectrum, portraying the VOC pattern of a specific sample. Peaks were detected by calculating local maxima. A propriety cluster analysis software (Purkhardt) was used to combine peaks with similar retention and drift times, assuming that every such combination represents a specific VOC. Unfortunately, there was no library to assign the different clusters to specific molecules.

3.7 Statistical analysis

The statistical analysis was performed using the IBM SPSS 25 software (IBM, Armonk, New York, United States).

For the description of data, measures of central tendency and dispersion were used in the form of mean, median, standard deviation, minimum, and maximum. Independent nominal variables were presented in a contingency table. For further investigation of relationships between the variables, the Mann-Whitney-U, Chi-squared, and Fisher exact tests were performed. A p-value of <0.05 was set as the level of statistical significance.

For the discriminant analysis of VOC-clusters measured by GC-IMS, a stepwise approach was used to select and eliminate variables from the model. This was done to improve

differentiation between groups in each step reflected by decreasing Wilks Lambda. The maximum significance level for including a variable from the model was 0.05 and the minimum significance level for elimination was 0.10. A maximum number of 106 steps could be performed by this method. The discriminant analysis was carried out in two parts, first for PCR positively tested patients (CT <40) and afterwards for patients categorized as contagious (CT <30). Afterwards, group classification results of the discriminant analysis were compared to those of the PCR test results.

To evaluate our model's performance, we did a cross-validation test. Typically, the data set is split into a training and a validation set, and the model is built using only the training set. The model is then used to make predictions on the validation set and calculate the mean squared error (MSE). The more accurate the predictions are, the smaller the MSE is. In our case, due to the small sample size, we decided on a specific form of cross-validation known as the leave-one-out method. Here, the training set consists of the whole data set except for one sample which constitutes the testing set. The training set is again used to build a model and to predict the value and MSE of the one sample of the testing set. This is repeated for every sample of the data set (85).

4. RESULTS

4.1 Descriptive analysis of the study population

After the exclusion process a total of 91 participants could be analysed. 49 of them were male (53.8%) with a mean age of 63.06 years and a standard deviation (SD) of 15.86. The youngest male participant was 23 years old, the oldest one 90. The remaining 42 female participants (46.2%) had a mean age of 61.64 years (SD: 22.75) and an age range from 22 to 88 years. Figure 20 shows the age distribution in males and females in a boxplot diagram. A rank sum test (Mann-Whitney-U) was conducted to assess the relationship between age and gender. No significant differences in age were found between males and females (z = -0.554, *P* = 0.580).

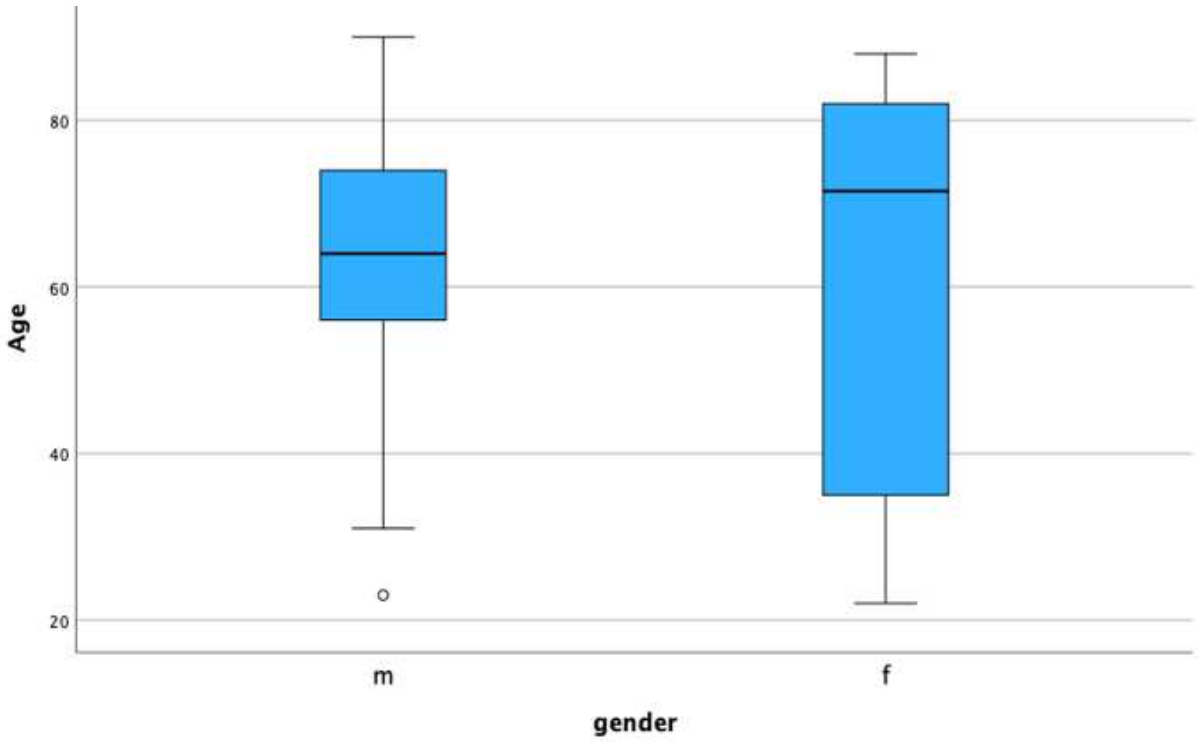

Figure 20. Boxplot diagram showing age distribution among genders

59 of 91 patients were tested positive for COVID-19 by a RT-qPCR test with a CT value below 40. The mean age among positively tested patients was 63.56 years (SD: 18.58) and 60.28 years among negatives (SD: 20.55), as shown in Figure 21. Again, a Mann-Whitney-U test was conducted showing no significant difference in age distribution between positively and negatively tested patients (z = -0.615, *P* = 0.538).

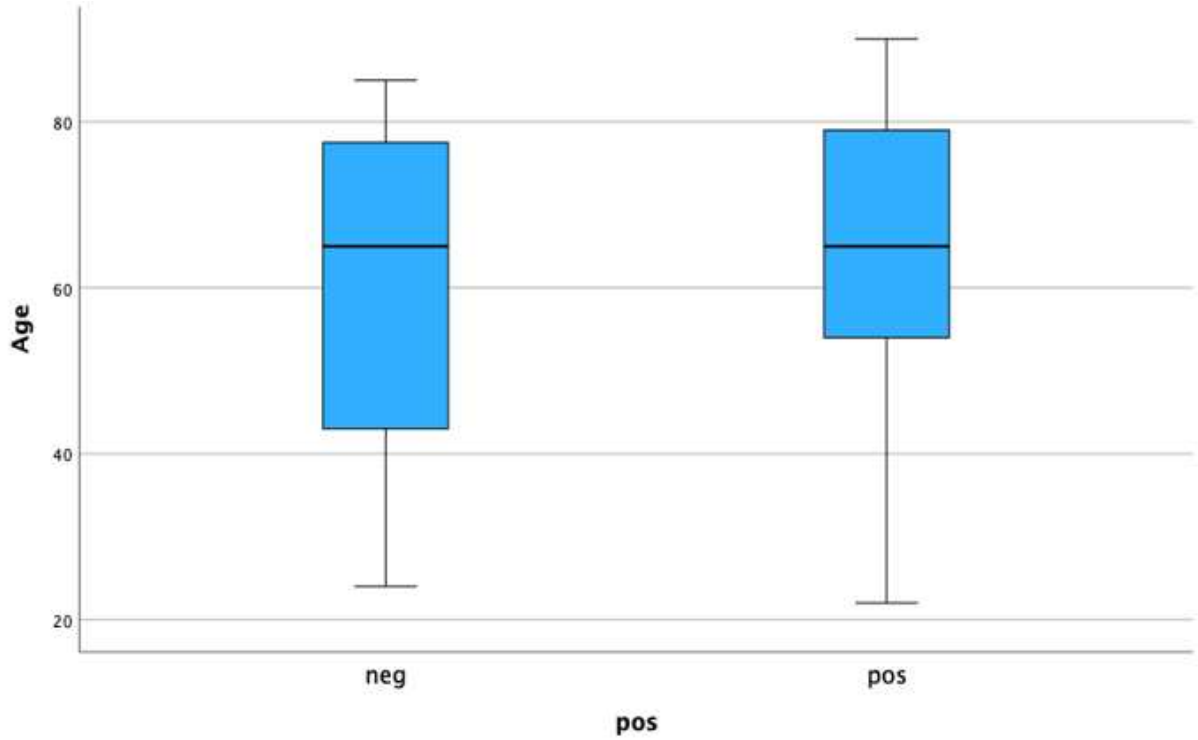

Figure 21. Boxplot diagram showing age distribution among positively and negatively tested patients

Table 2 shows the distribution of genders among the positive and negative groups. 35 of 59 positively tested patients were male (59.3%) and 24 female (40.7%). The remaining 32 negatives consisted of 14 male (43.7%) and 18 female (56.3%) patients.

Table 2. Gender distribution among study groups

			RT-qPCR		
Groups			**negative**	**positive**	**Total**
Gender	male	number	14	35	49
		percentage	43.7%	59.3%	53.8%
	female	number	18	24	42
		percentage	56.3%	40.7%	46.2%
Total		number	32	59	91
		Percentage	35.2%	64.8%	100%

In order to test the independence of the two variables we performed a Pearson's Chi-Square test and a Fisher's Exact test. The resulting p-values (Pearson Chi-Square: 0.155;

Fisher's Exact: 0.189 for two-sided, 0.115 for one-sided) showed no statistical significance, suggesting that there is no significant association between gender and the PCR test result.

4.2 Discriminant analysis of the VOC clusters

The cluster analysis of the GC-IMS spectra revealed 51 clusters, here listed as c1 to c51 in Table 3, together with their respective retention times (rt) and drift times (dt).

Table 3. List of VOC clusters

Cluster	rt* (s)	dt† (ms)	Cluster	rt (s)	dt (ms)
c1	20.02	39.90	**c27**	133.36	43.15
c2	15.86	7.57	**c28**	136.42	9.37
c3	22.05	14.17	**c29**	136.67	4.46
c4	21.91	20.72	**c30**	161.08	7.83
c5	28.21	3.24	**c31**	165.93	11.37
c6	25.21	28.45	**c32**	161.37	43.67
c7	41.24	22.88	**c33**	161.86	2.44
c8	34.13	34.36	**c34**	31.52	49.71
c9	33.99	64.31	**c35**	112.43	17.05
c10	48.70	44.10	**c36**	104.46	78.04
c11	45.30	8.84	**c37**	120.38	35.11
c12	51.02	28.90	**c38**	173.00	21.15
c13	50.94	16.94	**c39**	40.33	56.78
c14	56.01	51.97	**c40**	68.24	10.88
c15	84.72	43.10	**c41**	82.19	30.44
c16	68.63	5.09	**c42**	140.44	13.74
c17	86.45	8.96	**c43**	36.22	67.82
c18	89.45	20.04	**c44**	72.87	47.41
c19	99.97	13.74	**c45**	103.33	1.69
c20	87.53	24.62	**c46**	111.17	45.07
c21	102.50	97.50	**c47**	160.47	48.09
c22	107.61	41.64	**c48**	122.00	54.00
c23	116.16	7.84	**c49**	36.75	74.88
c24	117.26	21.85	**c50**	91.65	81.22
c25	134.57	19.84	**c51**	45.00	87.00
c26	126.81	29.58			

* rt = retention time in seconds
† dt = drift time in milliseconds

4.2.1 Comparison of VOC clusters to positively/negatively tested patients

In a stepwise canonical approach the clusters were added as variables to minimize Wilks Lambda. After inclusion of c20 and c40 no further minimization could be obtained using other parameters. A scatter plot was created to show the correlation between the two clusters and a positive or negative PCR test result (Figure 22).

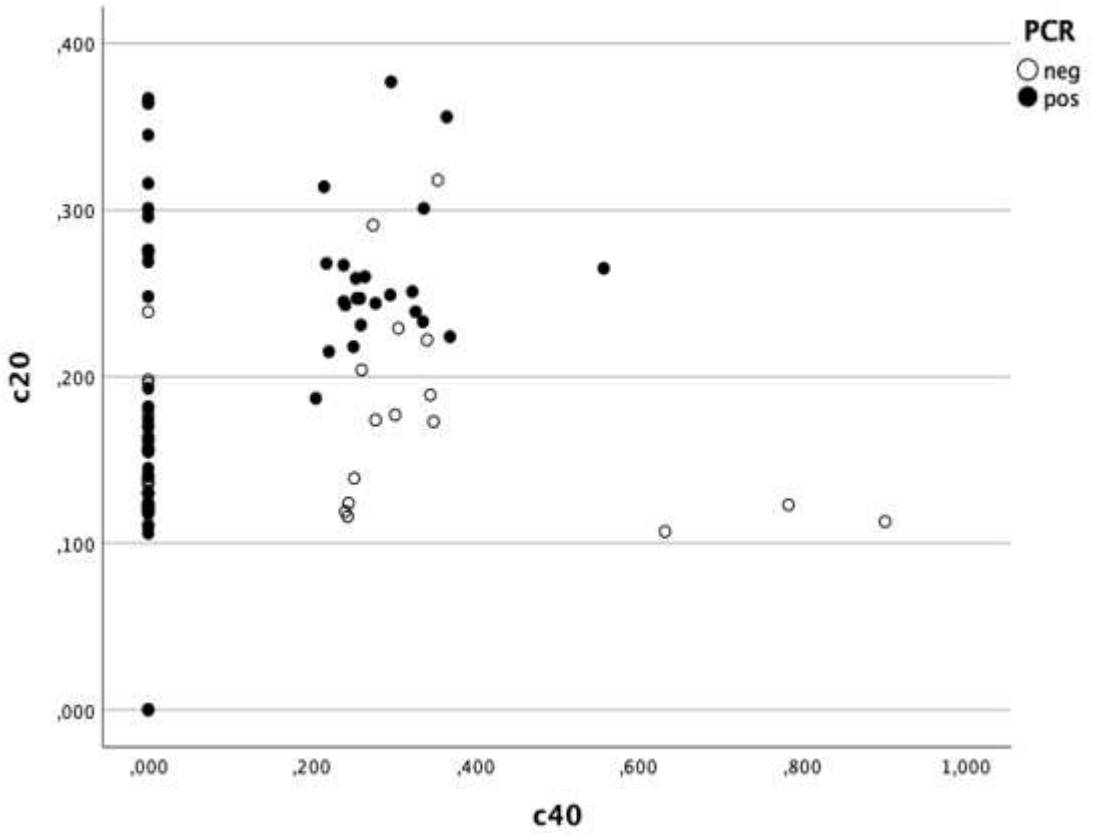

Figure 22. Correlation of c20 and c40 with PCR test results

Classification results comparing the predicted group affiliation with the the actual RT-qPCR test results, are shown in Table 4. 39 out of 59 patients were correctly classified as positive and 23 out of 32 as negative. Based on these numbers we could calculate the sensitivity and specificity of our method by the following formulas:

$$\text{Sensitivity} = [a / (a + c)] \times 100 = [39 / (39 + 20)] \times 100 = 66.1\%$$

$$\text{Specificity} = [d / (b + d)] \times 100 = [23 / (23 + 9)] \times 100 = 71.9\%$$

Overall 68.1% of cases were classified correctly with cross validation showing the same results.

A Chi-Square test (Chi^2 12.0, df = 1, P = 0,001) and a Fisher's Exact test (P = 0,001) showed a strong statistical significance.

Table 4. Classification results of VOC clusters in positive/negative patients

			Predicted group affiliation		
		PCR	**Positive**	**Negative**	**Total**
Original	Number	positive	39	20	59
		negative	9	23	32
	Percentage	positive	66.1	33.9	100
		negative	28.1	71.9	100
Cross validation	Number	positive	39	20	59
		negative	9	23	32
	Percentage	positive	66.1	33.9	100
		negative	28.1	71.9	100

4.2.2 Comparison of VOC clusters to contagious/noncontagious patients

Of 59 patients who were tested positively by RT-qPCR, 52 had CT values below 30 and were classified as contagious. 7 patients were categorized as positive, but not contagious, with their CT values ranging from 30.1 until 40. The same canonical discriminant analysis was performed in a stepwise approach, adding c20 in step 1 and c40 in step 2 to minimize Wilks Lamda.

Here, we calculated a sensitivity of 71.2% and a specificity of 59.0%. 65.9% of the initially grouped cases (original) and 64.8% of cross validated cases have been correctly classified. Another scatter plot was created as shown in Figure 23.

Again, we conducted a Chi-Square test (Chi^2 8.318, P = 0,004) and a Fisher's Exact test (P = 0,005), which also showed statistical significance.

Table 5. Classification results of VOC clusters in contagious/noncontagious patients

			Predicted group affiliation		
		CT	**Contagious**	**Non-contagious**	**Total**
Original	Number	Contagious	37	15	52
		Non-contagious	16	23	39
	Percentage	contagious	71.2	28.8	100
		Non-contagious	41.0	59.0	100
Cross validation	Number	contagious	37	15	52
		Non-contagious	17	22	39
	Percentage	contagious	71.2	28.8	100
		Non-contagious	43.6	56.4	100

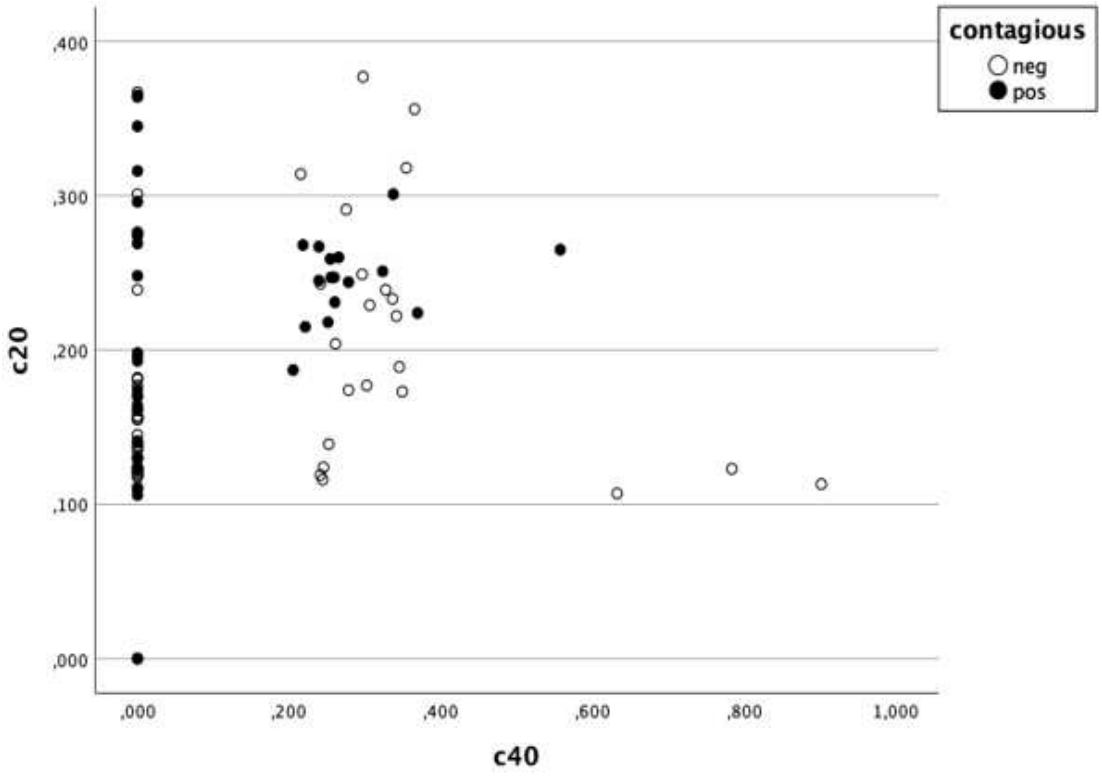

Figure 23. Correlation of c20 and c40 with contagiousness

5. DISCUSSION

In this study, we measured the VOC composition in the nasal breath of 91 patients of mixed age and gender with a GC-IMS device. Our goal was to find differences in VOC clusters between COVID-19 infected and non- infected patients.

49 of the 91 participants were male (53.8%) with 35 of them being tested positive by PCR (59.3%). Of the 42 female patients (46.2%) only 24 were tested positive (40.7%). Even though our results give the impression of a slighly higher rate of male hospitalized patients testing positive for SARS-CoV-2, the sample size was too small to confirm this and no statistically significant difference in gender has been found between the two groups (p-values: Pearson Chi-Square: 0.155; Fisher's Exact: 0.189 for two-sided, 0.115 for one-sided).

In the first part of our study, three VOC clusters obtained by exhaled breath through the oral cavity showed statistically relevant differences between positively and negatively tested patients (89). One of them, c20, conforms to our results of nasal measurement, raising the question of whether this is the cluster relevant for SARS-CoV-2 detection. The calculated sensitivity of GC-IMS was higher by oral measurement (78.9%) than by nasal (66.1%), whereas for specificity our calculated results were the same (71.9%). Considering the small sample size, the fact that the nasal measurement included two participants more than the oral may have led to these diverse results. On the other hand, after cross-validation of classification results in oral measurement the corrected sensitivity was only 68.8%, which is very close to the one of this study (66.1%).

In an earlier study using a multicapillary column coupled ion mobility spectrometer (MCC-IMS) device, Steppert *et al.* were able to additionally distinguish between SARS-CoV-2 and influenza-A infections. The MCC-IMS detected 155 clusters instead of 51 like in our case and 32 instead of two were needed in the stepwise approach to minimize Wilks Lambda. By that, 97.3% of the cases could be correctly classified, whereas in our study it was only 76.4% for oral and 68.1% for nasal measurement (65). Multiple factors may explain this difference. Firstly, Steppert's measurements took place during the wild- type phase of the pandemic whereas our study was conducted almost two years later. Other variants of concern with different characteristics and severity of symptoms, as well as a respectable part of the population being already immunized by previous COVID-19 infections or one or more doses of vaccines, could have likely played a role in type and degree of VOC expression during our measurements. Also, the MCC-IMS device works differently than our GC-IMS and may be able to measure more VOCs with a higher chance of finding specific clusters for COVID-19.

Also early during the pandemic, Ruszkiewicz *et al.* took breath samples of hospitalized patients in two locations, Edinburgh and Dortmund, and demonstrated that SARS-CoV-2 can

be detected by the use of GC-IMS. Some VOCs, distinguishing positive from negatively classified patients, could be identified. Those comprised aldehydes like ethanal, heptanal and octanal, ketones like acetone and butanone as well as methanol and an unidentified molecule (90). Unfortunately, due to lack of further analysis tools, it was not possible for us to identify our measured VOCs for a comparison. Nevertheless, for using our method as a screening tool, it is not necessary to know which exact molecules are being measured, but to detect them in the first place. Interestingly, the results for specificity (Edinburgh: 75%, Dortmund: 80%) were again relatively similar to ours, whereas sensitivity was higher (Edinburgh: 82.4%, Dortmund: 90%) (90). However, since it is not known whether the samples have been obtained via oral or nasal measurement, no true comparison is possible.

No studies were found on the VOC composition of contagious patients in comparison to non-contagious. Our goal hereby was to find out whether there are more and different VOC clusters with a higher viral load. For that we needed to set a cut-off at a CT value of 30 in order to distinguish contagious from non-contagious (but still positively tested) patients. In our stepwise approach the same VOC clusters were revealed, implicating that our method may not be suitable for assessing the phase and severity of disease, but rather the presence or absence of the infection. The same conclusion can be drawn from our results for sensitivity and specificity in measuring contagiousness. Even though sensitivity for contagiousness was slightly higher (71.2%) than for positivity, specificity was surprisingly low (59.0%). Considering that specificity is the ability of a test to correctly identify people without a condition, it is possible that VOC clusters are not much different in contagious and non-contagious, positive patients and it is therefore harder for the GC-IMS device to distinguish between the groups.

GC-IMS has several advantages over current testing strategies for SARS-CoV-2 and other viral infectious diseases. First of all, it is very fast (<5 minutes) and requires little consumables. During the pandemic it was soon clear that antigen tests were not fast and abundant enough for everyday testing of larger groups of people. Visitors at airports, hospitals, school children, employees in bigger companies etc. had to test themselves or get tested on a regular basis before being allowed to enter the buildings. Institutions had to trust them to perform the test, including a deep nasal swab, correctly and wait the full 15 minutes for the test result or they had to provide additional staff for testing. Long queues and people gathering due to waiting times raise the question whether this is the appropriate method to use in a pandemic.

In a systematic review, commercially available antigen tests have been grouped according to the type and location of the sample and evaluated by sensitivity and specificity.

Results showed that with a CT value of 25 or lower, sensitivity was very high (96%, 95%CI: 95-97), but decreased with higher CT values. Overall sensitivity was only 70% and therefore only slightly higher than that of GC-IMS in our study. However, overall specificity was very high with 98% (95%CI: 98-98).

Since antigen tests were not always readily available, other, more general screening methods were also often applied. These methods, including for example measuring the temperature of individuals before entering a public building, were very unspecific and could detect only symptomatic individuals of whom one would expect that they stayed at home anyways when not feeling well (91). The actual target group of screening methods, asymptomatic individuals, may not have had elevated body temperature and were therefore not detected. As said before, GC-IMS detects clusters of VOCs independently of state of disease and CT value and might offer a more reliable result than measuring temperature. Compared to antigen tests it is non-invasive and may be the more comfortable method to use, especially in children and elderly people. Nevertheless, further research has to be conducted and clusters identified which can definitely be attributed to SARS-CoV-2 in order for GC-IMS to become a reliable alternative to commonly used screening tools. As said before, GC-MS is already listed as an Emergency Use Authorization (EUA) product by the United States Food and Drug Administration (FDA) and may even be used as an individual diagnostic breath test and for the detection of COVID-19 by in “near patient / point-of-care” settings (84). For definite diagnosis after a positive screening result, RT-qPCR will remain the method of choice.

Limitations of the study included the small sample size as well as various confounding factors, namely the different history of patients regarding their vaccination status, previous COVID-19 infection, symptoms and severity of symptoms, time of infection, comorbidities, medication, nutrition and smoking as well as the VOC composition of surrounding air during measurement. Also, since we have no comparison group infected with another virus like Steppert *et al.*, we could not exclude that our measured VOC clusters are the host’s response to a general viral infection, instead of specific for SARS-CoV-2.

6. CONCLUSION

Patients, who tested positive for COVID-19 by PCR, can be detected by measuring the VOC composition in their nasal breath with GC-IMS.

This method provides an uncomplicated, fast, and non-invasive execution and does not need trained staff to perform. It is therefore suitable as a pre-screening tool for mass testing.

However, due to our small sample size and various confounding factors (different vaccination status, history of COVID-19 infection, symptoms and severity of symptoms, and time of infection) further research is necessary to confirm or even improve our results regarding sensitivity and specificity.

7. REFERENCES

1. Principles of Epidemiology | Lesson 1 - Section 11 [Internet]. 2023 [cited 2024 Aug 15]. Available from: https://archive.cdc.gov/www_cdc_gov/csels/dsepd/ss1978/lesson1/section11.html

2. Wolfe ND, Dunavan CP, Diamond J. Origins of major human infectious diseases. Nature. 2007;447(7142):279–83.

3. Weiss RA, Sankaran N. Emergence of epidemic diseases: zoonoses and other origins. Fac Rev. 2022;11:2.

4. Preventing and Preparing for Pandemics With Zoonotic Origins | Council on Foreign Relations [Internet]. [cited 2024 Aug 15]. Available from: https://www.cfr.org/report/preventing-and-preparing-pandemics-zoonotic-origins

5. Zoonotic & infectious disease | Center for One Health Research [Internet]. [cited 2024 Aug 15]. Available from: https://deohs.washington.edu/cohr/zoonotic-infectious-disease

6. Piret J, Boivin G. Pandemics Throughout History. Front Microbiol [Internet]. 2021 [cited 2024 Aug 15];11. Available from: https://www.frontiersin.org/journals/microbiology/articles/10.3389/fmicb.2020.631736/full

7. Zietz BP, Dunkelberg H. The history of the plague and the research on the causative agent *Yersinia pestis*. Int J Hyg Environ Health. 2004;207(2):165–78.

8. Johnson NPAS, Mueller J. Updating the accounts: global mortality of the 1918-1920 "Spanish" influenza pandemic. Bull Hist Med. 2002;76(1):105–15.

9. Sampath S, Khedr A, Qamar S, Tekin A, Singh R, Green R, et al. Pandemics Throughout the History. Cureus. 13(9):e18136.

10. Cascella M, Rajnik M, Aleem A, Dulebohn SC, Di Napoli R. Features, Evaluation, and Treatment of Coronavirus (COVID-19). In: StatPearls [Internet]. Treasure Island (FL): StatPearls Publishing; 2024 [cited 2024 Aug 15]. Available from: http://www.ncbi.nlm.nih.gov/books/NBK554776/

11. Carabelli AM, Peacock TP, Thorne LG, Harvey WT, Hughes J, COVID-19 Genomics UK Consortium, et al. SARS-CoV-2 variant biology: immune escape, transmission and fitness. Nat Rev Microbiol. 2023;21(3):162–77.

12. Justo Arevalo S, Castillo-Chávez A, Uribe Calampa CS, Zapata Sifuentes D, Huallpa CJ, Landa Bianchi G, et al. What do we know about the function of SARS-CoV-2 proteins? Front Immunol. 2023;14:1249607.

13. Zhang Q, Xiang R, Huo S, Zhou Y, Jiang S, Wang Q, et al. Molecular mechanism of interaction between SARS-CoV-2 and host cells and interventional therapy. Signal Transduct Target Ther. 2021;6(1):1–19.

14. Groß S, Jahn C, Cushman S, Bär C, Thum T. SARS-CoV-2 receptor ACE2-dependent implications on the cardiovascular system: From basic science to clinical implications. J Mol Cell Cardiol. 2020;144:47–53.

15. Teuwen LA, Geldhof V, Pasut A, Carmeliet P. COVID-19: the vasculature unleashed. Nat Rev Immunol. 2020;20(7):389–91.

16. PubChem. ACE2 - angiotensin converting enzyme 2 (human) [Internet]. [cited 2024 Aug 15]. Available from: https://pubchem.ncbi.nlm.nih.gov/gene/ACE2/human

17. Xiao L, Sakagami H, Miwa N. ACE2: The Key Molecule for Understanding the Pathophysiology of Severe and Critical Conditions of COVID-19: Demon or Angel? Viruses. 2020;12(5):491.

18. Beyerstedt S, Casaro EB, Rangel ÉB. COVID-19: angiotensin-converting enzyme 2 (ACE2) expression and tissue susceptibility to SARS-CoV-2 infection. Eur J Clin Microbiol Infect Dis. 2021;40(5):905–19.

19. Gary D. Hammer, Stephen J. McPhee. Pathophysiology of Disease An Introduction to Clinical Medicine. Eighth Edition. 2019. 337, 496–497 p.

20. van de Veerdonk FL, Netea MG, van Deuren M, van der Meer JW, de Mast Q, Brüggemann RJ, et al. Kallikrein-kinin blockade in patients with COVID-19 to prevent acute respiratory distress syndrome. eLife. 9:e57555.

21. Bryant JW, Shariat-Madar z. Human plasma kallikrein-kinin system: Physiological and biochemical parameters. Cardiovasc Hematol Agents Med Chem. 2009;7(3):234–50.

22. Shi S, Qin M, Cai Y, Liu T, Shen B, Yang F, et al. Characteristics and clinical significance of myocardial injury in patients with severe coronavirus disease 2019. Eur Heart J. 2020;ehaa408.

23. Guo T, Fan Y, Chen M, Wu X, Zhang L, He T, et al. Cardiovascular Implications of Fatal Outcomes of Patients With Coronavirus Disease 2019 (COVID-19). JAMA Cardiol. 20201;5(7):811–8.

24. Iwasaki M, Saito J, Zhao H, Sakamoto A, Hirota K, Ma D. Inflammation Triggered by SARS-CoV-2 and ACE2 Augment Drives Multiple Organ Failure of Severe COVID-19: Molecular Mechanisms and Implications. Inflammation. 2021;44(1):13–34.

25. Martinez-Rojas MA, Vega-Vega O, Bobadilla NA. Is the kidney a target of SARS-CoV-2? Am J Physiol - Ren Physiol. 2020;318(6):F1454–62.

26. Conway EM, Mackman N, Warren RQ, Wolberg AS, Mosnier LO, Campbell RA, et al. Understanding COVID-19-associated coagulopathy. Nat Rev Immunol. 2022;22(10):639–49.

27. Cesari M, Pahor M, Incalzi RA. PLASMINOGEN ACTIVATOR INHIBITOR-1 (PAI-1): A KEY FACTOR LINKING FIBRINOLYSIS AND AGE-RELATED SUBCLINICAL AND CLINICAL CONDITIONS. Cardiovasc Ther. 2010;28(5):e72–91.

28. Burstein SA. Effects of interleukin 6 on megakaryocytes and on canine platelet function. Stem Cells Dayt Ohio. 1994;12(4):386–93.

29. COVID-19 Treatment Guidelines [Internet]. [cited 2024 Aug 16]. Information on COVID-19 Treatment, Prevention and Research. Available from: https://www.covid19treatmentguidelines.nih.gov/

30. Nishiura H, Kobayashi T, Miyama T, Suzuki A, Jung S mok, Hayashi K, et al. Estimation of the asymptomatic ratio of novel coronavirus infections (COVID-19). Int J Infect Dis. 2020;94:154–5.

31. CDC. COVID-19. 2024 [cited 2024 Aug 15]. Overview of Testing for SARS-CoV-2. Available from: https://www.cdc.gov/covid/hcp/testing/index.html

32. Shreffler J, Huecker MR. Diagnostic Testing Accuracy: Sensitivity, Specificity, Predictive Values and Likelihood Ratios. In: StatPearls [Internet]. Treasure Island (FL): StatPearls Publishing; 2024 [cited 2024 Aug 15]. Available from: http://www.ncbi.nlm.nih.gov/books/NBK557491/

33. Molecular Biology of PCR Testing for COVID-19 Diagnostics | IntechOpen [Internet]. [cited 2024 Aug 15]. Available from: https://www.intechopen.com/chapters/75245

34. Dorta-Gorrín A, Navas-Méndez J, Gozalo-Margüello M, Miralles L, García-Hevia L. Detection of SARS-CoV-2 Based on Nucleic Acid Amplification Tests (NAATs) and Its Integration into Nanomedicine and Microfluidic Devices as Point-of-Care Testing (POCT). Int J Mol Sci. 2023;24(12):10233.

35. Rapid, point-of-care antigen tests for diagnosis of SARS-CoV-2 infection - PMC [Internet]. [cited 2024 Aug 15]. Available from: https://www.ncbi.nlm.nih.gov/pmc/articles/PMC9305720/

36. https://www.who.int/docs/default-source/coronaviruse/real-time-rt-pcr-assays-for-the-detection-of-sars-cov-2-institut-pasteur-paris.pdf [Internet]. [cited 2024 Aug 18]. Available from: https://www.who.int/docs/default-source/coronaviruse/real-time-rt-pcr-assays-for-the-detection-of-sars-cov-2-institut-pasteur-paris.pdf

37. Dutta D, Naiyer S, Mansuri S, Soni N, Singh V, Bhat KH, et al. COVID-19 Diagnosis: A Comprehensive Review of the RT-qPCR Method for Detection of SARS-CoV-2. Diagnostics. 2022;12(6):1503.

38. admin.facellitate. Advantages and disadvantages of PCR technology [Internet]. faCellitate. 2023 [cited 2024 Aug 15]. Available from: https://facellitate.com/advantages-and-disadvantages-of-pcr-technology/

39. EUR-Lex - 02010L0075-20110106 - EN - EUR-Lex [Internet]. [cited 2024 Aug 15]. Available from: https://eur-lex.europa.eu/eli/dir/2010/75/2011-01-06/eng

40. US EPA O. Technical Overview of Volatile Organic Compounds [Internet]. 2014 [cited 2024 Aug 15]. Available from: https://www.epa.gov/indoor-air-quality-iaq/technical-overview-volatile-organic-compounds

41. US EPA O. What are volatile organic compounds (VOCs)? [Internet]. 2019 [cited 2024 Aug 15]. Available from: https://www.epa.gov/indoor-air-quality-iaq/what-are-volatile-organic-compounds-vocs

42. Deuscher Z, Gourrat K, Repoux M, Boulanger R, Labouré H, Le Quéré JL. Key Aroma Compounds of Dark Chocolates Differing in Organoleptic Properties: A GC-O Comparative Study. Mol Basel Switz. 2020;25(8):1809.

43. Pandey P, Yadav R. A Review on Volatile Organic Compounds (VOCs) as Environmental Pollutants: Fate and Distribution. Int J Plant Environ. 2018;4.

44. StudySmarter UK [Internet]. [cited 2024 Aug 16]. Organic Compounds: Definition & Examples | StudySmarter. Available from: https://www.studysmarter.co.uk/explanations/chemistry/organic-chemistry/organic-compounds/

45. Organic compounds Classification, Functional group and Homologous series [Internet]. Online Chemistry notes. 2020 [cited 2024 Aug 16]. Available from: https://chemicalnote.com/organic-compounds-classification-functional-group-and-homologous-series/

46. Encyclopedia of Toxicology. Third. Vol. 1. Philip Wexler; 2014.

47. Functional Groups in Organic Compounds [Internet]. Compound Interest. 2014 [cited 2024 Aug 16]. Available from: https://www.compoundchem.com/2014/01/24/functional-groups-in-organic-compounds/

48. Socratic.org [Internet]. [cited 2024 Aug 16]. What is a halogen atom? | Socratic. Available from: https://socratic.org/questions/what-is-a-halogen-atom

49. Chemistry LibreTexts [Internet]. 2014 [cited 2024 Aug 16]. 14.9: Aldehydes and Ketones- Structure and Names. Available from: https://chem.libretexts.org/Bookshelves/Introductory_Chemistry/Basics_of_General_Organic_and_Biological_Chemistry_(Ball_et_al.)/14%3A_Organic_Compounds_of_Oxygen/14.09%3A_Aldehydes_and_Ketones-_Structure_and_Names

50. AQT [Internet]. [cited 2024 Aug 16]. Complete list of VOC's. Available from: https://aqt-vru.com/emissions/complete-list-of-vocs/

51. https://neomeditec.com/VOCdatabase/first-page/ [Internet]. VOC Biomarkers Database. [cited 2024 Aug 16]. Available from: https://neomeditec.com/VOCdatabase/first-page/

52. Volatile organic compounds emitted by humans indoors– A review on the measurement, test conditions, and analysis techniques - ScienceDirect [Internet]. [cited 2024 Aug 16]. Available from: https://www.sciencedirect.com/science/article/pii/S0360132324002841

53. The Internet Classics Archive | Aphorisms by Hippocrates [Internet]. [cited 2024 Aug 16]. Available from: https://classics.mit.edu/Hippocrates/aphorisms.html

54. Shirasu M, Touhara K. The scent of disease: volatile organic compounds of the human body related to disease and disorder. J Biochem (Tokyo). 2011;150(3):257–66.

55. Pauling L, Robinson AB, Teranishi R, Cary P. Quantitative Analysis of Urine Vapor and Breath by Gas-Liquid Partition Chromatography. Proc Natl Acad Sci U S A. 1971;68(10):2374–6.

56. de Lacy Costello B, Amann A, Al-Kateb H, Flynn C, Filipiak W, Khalid T, et al. A review of the volatiles from the healthy human body. J Breath Res. 2014;8(1):014001.

57. Filipiak W, Mochalski P, Filipiak A, Ager C, Cumeras R, Davis CE, et al. A Compendium of Volatile Organic Compounds (VOCs) Released By Human Cell Lines. Curr Med Chem. 2016;23(20):2112–31.

58. Tez M, Şahingöz E, Martli F. Advancements in Breath-Based Diagnostics for Pancreatic Cancer: Current Insights and Future Perspectives. World J Gastrointest Oncol. 2024;16.

59. Alsaadi D, Clements N, Gabuniya N, Francis N, Chand M. Exhaled volatile organic compounds in the detection of colorectal cancer: a systematic review and meta-analysis. EXCLI J. 2024;23:795–810.

60. Fan X, Zhong R, Liang H, Zhong Q, Huang H, He J, et al. Exhaled VOC detection in lung cancer screening: a comprehensive meta-analysis. BMC Cancer. 2024;24.

61. Mochalski P, King J, Haas M, Unterkofler K, Amann A, Mayer G. Blood and breath profiles of volatile organic compounds in patients with end-stage renal disease. BMC Nephrol. 2014;15:43.

62. Sehnert S, Jiang L, Burdick J, Risby T. Breath biomarkers for detection of human liver diseases: Preliminary study. Biomark Biochem Indic Expo Response Susceptibility Chem. 2002;7:174–87.

63. (PDF) Fecal Volatile Organic Compounds and Microbiota Associated with the Progression of Cognitive Impairment in Alzheimer's Disease [Internet]. [cited 2024 Aug 17]. Available from: https://www.researchgate.net/publication/366831425_Fecal_Volatile_Organic_Compounds_and_Microbiota_Associated_with_the_Progression_of_Cognitive_Impairment_in_Alzheimer%27s_Disease

64. Rapid in vitro differentiation of bacteria by ion mobility spectrometry [Internet]. [cited 2024 Aug 17]. Available from: http://ouci.dntb.gov.ua/en/works/4ERWryAl/

65. Steppert C, Steppert I, Sterlacci W, Bollinger T. Rapid detection of SARS-CoV-2 infection by multicapillary column coupled ion mobility spectrometry (MCC-IMS) of breath. A proof of concept study. J Breath Res. 2021;15(2).

66. Steppert C, Steppert I, Bollinger T, Sterlacci W. Rapid non-invasive detection of Influenza-A-infection by multicapillary column coupled ion mobility spectrometry. J Breath Res. 2020;15(1):011001.

67. Haick H, Broza YY, Mochalski P, Ruzsanyi V, Amann A. Assessment, origin, and implementation of breath volatile cancer markers. Chem Soc Rev. 2014;43(5):1423–49.

68. Zhao RZ, Jiang S, Zhang L, Yu ZB. Mitochondrial electron transport chain, ROS generation and uncoupling (Review). Int J Mol Med. 2019;44(1):3–15.

69. Liu Z, Ren Z, Zhang J, Chuang CC, Kandaswamy E, Zhou T, et al. Role of ROS and Nutritional Antioxidants in Human Diseases. Front Physiol. 2018;9:477.

70. Aksenov AA, Gojova A, Zhao W, Morgan JT, Sankaran S, Sandrock CE, et al. Characterization of Volatile Organic Compounds in Human Leukocyte Antigen

Heterologous Expression Systems: a Cell's "Chemical Odor Fingerprint." ChemBioChem. 2012;13(7):1053–9.

71. Cruz-Tapias P, Castiblanco J, Anaya JM. Major histocompatibility complex: Antigen processing and presentation. In: Autoimmunity: From Bench to Bedside [Internet] [Internet]. El Rosario University Press; 2013 [cited 2024 Aug 16]. Available from: https://www.ncbi.nlm.nih.gov/books/NBK459467/

72. Clark DW, Palle K. Aldehyde dehydrogenases in cancer stem cells: potential as therapeutic targets. Ann Transl Med. 2016;4(24):518.

73. Brunner C, Szymczak W, Höllriegl V, Mörtl S, Oelmez H, Bergner A, et al. Discrimination of cancerous and non-cancerous cell lines by headspace-analysis with PTR-MS. Anal Bioanal Chem. 2010;397(6):2315–24.

74. Introduction to Gas Chromatography—Principles, Characteristics, and Process [Internet]. Creative Proteomics Blog. 2020 [cited 2024 Aug 16]. Available from: https://www.creative-proteomics.com/blog/introduction-to-gas-chromatography-principles-characteristics-and-process/

75. Overview of GC [Internet]. [cited 2024 Aug 16]. Available from: https://www.shimadzu.com/an/service-support/technical-support/analysis-basics/fundamentals/gc.html

76. Smolinska A, Hauschild AC, Fijten R, Dallinga J, Baumbach J, Van Schooten F. Current breathomics - A review on data pre-processing techniques and machine learning in metabolomics breath analysis. J Breath Res. 2014;8:027105.

77. Analysis & Separations from Technology Networks [Internet]. [cited 2024 Aug 16]. GC-MS Principle, Instrument and Analyses and GC-MS/MS. Available from: http://www.technologynetworks.com/analysis/articles/gc-ms-principle-instrument-and-analyses-and-gc-msms-362513

78. analyticon - handheld power [Internet]. [cited 2024 Aug 16]. analyticon - handheld power. Available from: https://www.analyticon.eu/en/ion-mobility-spectrometry.html

79. Dodds JN, Baker ES. Ion Mobility Spectrometry: Fundamental Concepts, Instrumentation, Applications, and the Road Ahead. J Am Soc Mass Spectrom. 2019;30(11):2185–95.

80. Moura PC, Raposo M, Vassilenko V. Breath volatile organic compounds (VOCs) as biomarkers for the diagnosis of pathological conditions: A review. Biomed J. 2023;46(4):100623.

81. Yin J, Wu M, Lin R, Li X, Ding H, Han L, et al. Application and development trends of gas chromatography–ion mobility spectrometry for traditional Chinese medicine, clinical, food and environmental analysis. Microchem J. 2021;168:106527.

82. Parastar H, Weller P. Towards greener volatilomics: Is GC-IMS the new Swiss army knife of gas phase analysis? TrAC Trends Anal Chem. 2023;170:117438.

83. Yang X, Zhang T, Yang D, Xie J. Application of gas chromatography-ion mobility spectrometry in the analysis of food volatile components. Acta Chromatogr. 2022;35.

84. Health C for D and R. In Vitro Diagnostics EUAs - Other Tests for SARS-CoV-2. FDA [Internet]. 2023 [cited 2024 Aug 16]; Available from: https://www.fda.gov/medical-devices/covid-19-emergency-use-authorizations-medical-devices/in-vitro-diagnostics-euas-other-tests-sars-cov-2

85. Bobbitt Z. Statology. 2020 [cited 2024 Aug 16]. A Quick Intro to Leave-One-Out Cross-Validation (LOOCV). Available from: https://www.statology.org/leave-one-out-cross-validation/

86. Fabião J, Sassi B, Pedrollo EF, Gerchman F, Kramer CK, Leitão CB, et al. Why do men have worse COVID-19-related outcomes? A systematic review and meta-analysis with sex adjusted for age. Braz J Med Biol Res. 2022;55:e11711.

87. Schurz H, Salie M, Tromp G, Hoal EG, Kinnear CJ, Möller M. The X chromosome and sex-specific effects in infectious disease susceptibility. Hum Genomics. 2019;13:2.

88. Sama IE, Ravera A, Santema BT, van Goor H, Ter Maaten JM, Cleland JGF, et al. Circulating plasma concentrations of angiotensin-converting enzyme 2 in men and women

with heart failure and effects of renin-angiotensin-aldosterone inhibitors. Eur Heart J. 2020;41(19):1810–7.

89. Molitor TB. Detection of COVID-19 infection in exhaled breath by gas chromatography coupled ion mobility spectrometry (GC-IMS) [Internet] [info:eu-repo/semantics/masterThesis]. University of Split. School of Medicine; 2023 [cited 2024 Aug 17]. Available from: https://urn.nsk.hr/urn:nbn:hr:171:334238

90. Ruszkiewicz DM, Sanders D, O'Brien R, Hempel F, Reed MJ, Riepe AC, et al. Diagnosis of COVID-19 by analysis of breath with gas chromatography-ion mobility spectrometry - a feasibility study. eClinicalMedicine [Internet]. 2020 [cited 2024 Aug 17];29. Available from: https://www.thelancet.com/journals/eclinm/article/PIIS2589-5370(20)30353-9/fulltext

91. Dell'Isola GB, Cosentini E, Canale L, Ficco G, Dell'Isola M. Noncontact Body Temperature Measurement: Uncertainty Evaluation and Screening Decision Rule to Prevent the Spread of COVID-19. Sensors. 2021;21(2):346.

8. SUMMARY

Objectives: This study was aimed to assess whether GC-IMS can be used for the detection of SARS-CoV-2.

Methods: We performed a non-randomized controlled study measuring VOC clusters in the nasal breath of 91 hospitalized patients with a GC-IMS device. The study was conducted at the Regiomed hospital Coburg between April and July 2022. Patients were divided into two groups, according to their PCR test result (CT <40) and were measured with GC-IMS not longer than 24 hours after their PCR test. Participants needed to give their written informed consent and meet the inclusion criteria for our study. Statistical analysis in form of data descriptive tests (Mann-Whitney-U, Pearson's Chi-squared and Fisher's exact) and discriminant cluster analysis of the measured VOCs (stepwise canonical approach, leave-one-out cross validation) was performed using IBM SPSS 25.

Results: There were no statistically significant findings regarding age distribution among genders and study groups. 51 clusters were measured by GC-IMS in the nasal breath of patients; 2 clusters showed statistically relevant differences among the study groups. GC-IMS correctly classified 68.1% of patients regarding their PCR test result and 65.9% (64.8% after cross validation) regarding their contagiousness (CT <30). Based on that we calculated a sensitivity of 66.1% and specificity of 71.9% for GC-IMS.

Conclusion: GC-IMS can detect SARS-CoV-2 by measuring the VOC composition of patients' nasal breath with a sensitivity similar to those of antigen tests. It may therefore serve as a cost-effective, fast and non-invasive screening method, especially at places where mass testing is required.

9. CROATIAN SUMMARY

Naslov: OTKRIVANJE INFEKCIJE COVID-19 U NOSNOM DAHU POMOĆU PLINSKE KROMATOGRAFIJE SPOJENE S IONSKOM SPEKTROMETRIJOM (GC-IMS)

Ciljevi: Ova studija je imala za cilj procijeniti može li se GC-IMS koristiti za otkrivanje SARS-CoV-2.

Materijali i metode: Proveli smo nekontroliranu, nenamjensku studiju mjereći VOC skupine u nosnom dahu 91 hospitaliziranog pacijenta pomoću GC-IMS uređaja. Studija je provedena u bolnici Regiomed u Coburgu između travnja i srpnja 2022. Pacijenti su bili podijeljeni u dvije skupine, prema rezultatu njihovog PCR testa (CT <40) i mjerili su se s GC-IMS ne duže od 24 sata nakon PCR testa. Sudionici su trebali dati svoj pisani informirani pristanak i ispuniti kriterije inkluzije za našu studiju. Statistička analiza u obliku deskriptivnih testova podataka (Mann-Whitney U, Pearsonov hi-kvadrat i Fisherova egzaktna) i diskriminantna klasterska analiza izmjerenih VOC-ova (korak po korak kanonski pristup, leave-one-out unakrsna validacija) provedena je korištenjem IBM SPSS 25.

Rezultati: Nisu zabilježeni statistički značajni nalazi u vezi s distribucijom dobi među spolovima i istraživačkim skupinama. 51 klaster mjerena je metodom GC-IMS u nosnom dahu pacijenata; 2 klastera pokazala su statistički relevantne razlike među istraživačkim skupinama. GC-IMS ispravno je klasificirao 68,1% pacijenata prema rezultatu njihovog PCR testa i 65,9% (64,8% nakon unakrsne validacije) prema njihovoj zaraznosti (CT <30). Na temelju toga izračunali smo senzitivnost od 66,1% i specifičnost od 71,9% za GC-IMS.

Zaključci: GC-IMS može otkriti SARS-CoV-2 mjereći sastav VOC-a u nosnom dahu pacijenata sa senzitivnošću sličnom onima antigenskih testova. Stoga može poslužiti kao isplativa, brza i neinvazivna metoda skrininga, posebno na mjestima gdje je potrebno masovno testiranje.